Carbon isotopic composition of plant-derived organic matter in tropical sedimentary sequences as a recorder of Late Cretaceous-Early Paleogene changes in the carbon cycle

by

Humberto Carvajal-Ortiz

A thesis submitted to the graduate faculty
in partial fulfillment of the requirements for the degree of
MASTER OF SCIENCE

Major: Geology

Program of Study Committee:
German Mora, Major Professor
William Jenks
Jiasong Fang

Iowa State University
Ames, Iowa
2007

DEDICATORY

In general, I want to thank my family and friends. Thanks for the love and support. I want to specially thank my mother, Sara, and my sister, Ruth, because they have been right by my side…always. Thanks to Dr. German Mora, my mentor and infinite source of knowledge, I have nothing but immense gratitude to you. Thanks to God almighty. Finally, I want to not only thank, but also to express my infinite love to the person who has been my sunrise and sunset, my muse, my southern star…Thank you, my Jenny.

TABLE OF CONTENTS

ACKNOWLEDGMENTS

I would like to give my thanks to the organizations that funded this research. Thanks to the Geological Society of America for providing partial financial support (Grant number 8229-06) and to the Center for Global and Regional Environmental Research at the University of Iowa for partially funding this research, as well. I would also like to thank everyone who helped me completing my research and my thesis. First of all, thanks to my advisor, Dr. German Mora, for his advice and help in this research, his patience, and infinite knowledge. Thanks to Dr. Jiasong Fang for allowing me to use the GCMS instrumentation of the Biogeochemistry lab, for being my teacher, and for being a committee member in my thesis. Thanks to Dr. William Jenks for the knowledge he shared during his class and also for being a committee member. Thanks to my fellow graduate student, Jin Zhang, for her assistance and emotional support. Thanks to Dr. Steve Veysey, for his help during the biomarker analysis at the Chemical Instrumentation Facility center of the Chemistry Department. Thanks to Dr. Carl Jacobson for his support when needed. Thanks to DeAnn Frisk for her efficient work, for keeping everything in order, and for receiving all my mail (a lot). Thanks to Dr. Paul Spry for his advice and support. Finally, I would like to thank Dr. Carlos Jaramillo and the Colombian Petroleum Institute (ICP) for providing the samples for this study.

ABSTRACT

The dynamics associated with the carbon cycle and the linkage between the oceans, the atmosphere, and land plants provide an opportunity to correlate marine and terrestrial sedimentary sequences using stable isotopes of carbon ($\delta^{13}C$), but few studies have tested this approach. To evaluate the possibility of using carbon isotope ratios of bulk sedimentary organic matter derived from land plants ($\delta^{13}C_{bulk}$) as a chronostratigraphic tool, we are comparing the composite Paleocene-Eocene marine carbon-isotope ($\delta^{13}C_{carbonate}$) record from Zachos et al., (2001) to that of a terrestrial sequence from Colombia. Sediments of the terrestrial rock units were deposited in a transitional setting dominated by mudstones, coals, and small lenses of sandstones (Catatumbo and Barco Formations) and in a mixture of deltaic and fluvial conditions (Cuervos Formation). The stratigraphic control was based on palynological zones for the region. The $\delta^{13}C_{bulk}$ values for the studied terrestrial sequence show three carbon-isotope excursions, which correlate closely with those present in the marine record. The $\delta^{13}C_{bulk}$ values decreased from -24‰ to -26.5‰ in sediments accumulated during early to middle Paleocene. This shift is commonly associated with the slow recovery in marine primary production that occurred in the aftermath of the extinction event of the Cretaceous-Tertiary boundary. The positive shift in sediments accumulated during the late Paleocene shows $\delta^{13}C_{bulk}$ values increasing from -26.5‰ to -23.8‰. This event is commonly associated with the burial of large amounts of organic matter. The third excursion is found near the Paleocene-Eocene boundary, with values changing from -23.8‰ to -26.5‰. This

shift is commonly interpreted to result from a long-term trend toward higher temperatures (52-50 million years ago, M.a.). The analysis of selected biomarker ratios (CPI, Pr/Ph, Paq, ββ/ββ+αβ hopanes) shows some diagenetic transformation. However, no correlation between diagenesis and $\delta^{13}C_{bulk}$ values was detected, thus suggesting that $\delta^{13}C_{bulk}$ could be correlated with $\delta^{13}C_{carbonate}$ values. The close correspondence that was found between $\delta^{13}C_{bulk}$ and $\delta^{13}C_{carbonate}$ values provides support to the hypothesis that a tight land plant-oceans linkage exists through geologic timescales via the atmosphere.

1. INTRODUCTION

Significant changes in both marine and terrestrial environments have occurred during the Phanerozoic (since 540 M.a.). For example, significant stagnation in the oceans during particular intervals in the Mesozoic (oceanic anoxic events) resulted in the widespread accumulation of black shales (Jenkyns, 2003). On land, pollen data show that major extinction events affected terrestrial vegetation during the Mesozoic and Cenozoic (Harrington and Jaramillo, 2007). Although occurring in different settings, these events and others have in common that they alter the carbon cycle by, for example, sequestering organic carbon in marine shales (i.e., oceanic anoxic events) decreases the amount of atmospheric CO_2 (land plants photosynthesis) over short time scales (<1 million years, M.y.). These changes in the carbon cycle are likely to be global in scale, thus potentially offering an opportunity to correlate marine and terrestrial sedimentary sequences, which at the moment is limited to a few approaches. Because of the potential linkage between marine and terrestrial realms through the carbon cycle, some studies have proposed the use of stable isotopes of carbon to correlate marine and terrestrial sequences (Gröcke, 1998; Arens and Jahren, 2000; Strauss and Peters-Kottig, 2003). The overall objective of this study is to test the hypothesis that the isotopic composition of plant-derived sedimentary organic matter has been affected by changes in the isotopic composition of the oceans, thus allowing the use of this proxy for correlation purposes.

1.1. THE CARBON CYCLE

Carbon is continuously transferred from different compartments on Earth, including the atmosphere, the biosphere (marine and terrestrial plants), the hydrosphere, and the lithosphere (Tissot and Welte, 1984) (Figure 1). Because the residence time of carbon in each compartment varies (Figure 1), the carbon cycle is commonly subdivided into two sub-cycles: the short and long-term cycles (Tissot and Welte, 1984), with residence times averaging 1000 years and tens to hundreds millions of years, respectively (Tissot and Welte, 1984; Killops and Killops, 2005).

Over geologic time scales (long-term cycle), the residence time and the magnitude of carbon fluxes have not been constant through time, as a result of perturbations inside the cycle (Weissert et al., 1998; Veizer et al., 1999; Gröcke et al., 1999; Thomas et al., 2002; Strauss and Peters-Kottig, 2003; Hollis et al., 2005; Jahren et al., 2005). For example, human activities, including fossil-fuel combustion and land-use changes, have induced rapid changes in the carbon cycle by transferring carbon stored in sedimentary rocks and soils to the atmosphere. Not only has this process produced higher CO_2 concentrations in the atmosphere, but it has also increased mean global temperatures (Petit et al., 1999; Rost, 2003). This modern alteration of the carbon cycle serves as a modern analog to explain how these changes could be recorded globally and, then, allow terrestrial and marine sequences to be correlated with the aid of carbon isotope ratios.

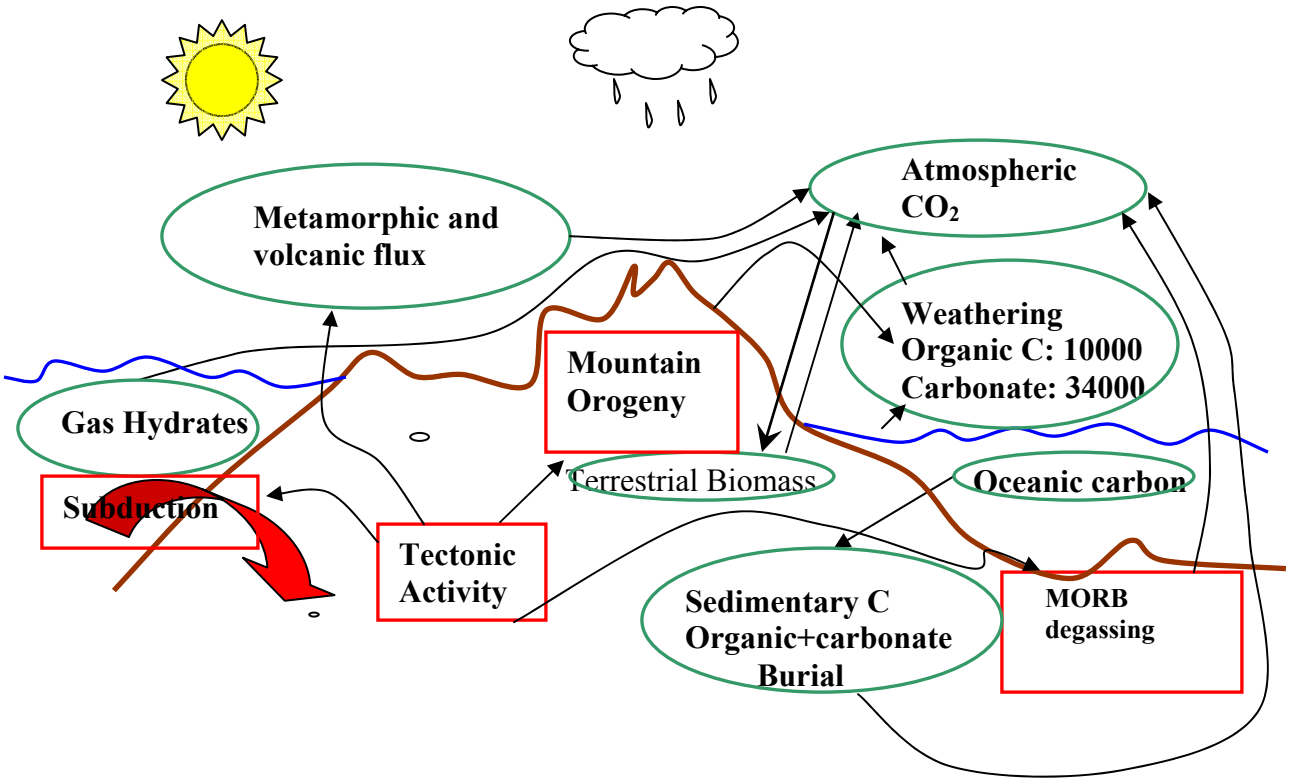

Figure 1. The carbon cycle showing reservoirs (green ovals) and fluxes (red squares) (after Kump and Arthur, 1999).

During the combustion of fossil fuels a preferential enrichment of ^{12}C in atmospheric CO_2 occurs because of the more negative isotopic composition (^{12}C-enriched) of fossil fuels, thus generating an isotopic signature for this process. For example, the isotopic composition of oceans has progressively become more ^{12}C-enriched since the Industrial Revolution (Böhm et al., 1996) as it has been observed in marine carbonates.

The abundance of stable isotopes is reported using the following notation:

$$\delta^{13}C = (^{13}R_{sample} / {}^{13}R_{standard} - 1)* 1000 \quad (1)$$

Where, ^{13}R is the $^{13}C/^{12}C$ ratio in both the standard and the sample. The notation is expressed in per thousand or per mil (‰). The standard is a carbonate shell of belemnite fossils (a mollusk) found in limestones of the Peedee Formation in South Carolina, USA. This limestone has an accepted ^{13}R value of 0.01124 (Craig, 1953).

Following the reasoning that carbon-transferring process carry their own isotopic signature, several research studies have attempted to track carbon isotopic anomalies throughout the geologic history using the isotopic signature recorded in marine carbonates and sedimentary organic matter, and link them with their possible triggering processes (Weissert and Erba, 2004; Gröcke et al., 1999; Veizer et al., 1999; Thomas et al., 2002; Hollis et al., 2005; Jahren et al., 2005). A good example of a secular variation affecting the carbon cycle is reported by Zachos et al. (2001) and Thomas et al. (2002), who identified a negative anomaly of ~ -4‰ recorded in marine planktonic and benthonic foraminifera accumulated during the Paleocene-Eocene boundary. This anomaly resulted from the release of significant amounts of methane from continental margins. Similarly, periods of unusual carbon transfer between compartments associated with increasing volcanic activity (Hesselbo et al., 2002), land plant evolution (Freeman and Colarusso, 2001), and mass extinctions of primary producers (Arens and Jahren, 2000; Kaiser et al., 2006; Berner, 2006) have

been documented in the geologic past, and all of them are associated with changes in the isotopic composition of both marine and terrestrial carbon (Koch et al., 1992 and 1998; Gröcke, 1998; Berner, 2006). Marine carbonates record this partitioning of isotopes because such secular changes affect the functioning of the marine carbon pumps (Rost et al., 2002), which in turn affect the distribution of the dissolved inorganic carbon (DIC) and ultimately $\delta^{13}C_{Carbonate}$ values. These isotopic values, in turn, are dependent on the carbon chemistry of the oceans.

1.1.1. OCEAN CARBON GEOCHEMISTRY

The transfer of atmospheric CO_2 into the oceans and vice versa is driven by physicochemical and biological processes called physical and biological carbon pumps, respectively, which drives the vertical distribution of the dissolved inorganic carbon (DIC) species (Rost et al., 2003; Killops and Killops, 2005; van Breugel, 2006). When CO_2 dissolves in oceans, a series of equilibrium reactions takes place, which lead to the formation of all the DIC species:

$$\mathbf{CO_{2\,(g)} \longleftrightarrow CO_{2\,(d)} \longleftrightarrow H_2CO_3 \longleftrightarrow HCO_3^- \longleftrightarrow CO_3^{2-}} \quad \mathbf{(2)}$$

Where, $CO_{2\,(g)}$ is atmospheric carbon dioxide, $CO_{2\,(d)}$ is dissolved carbon dioxide, H_2CO_3 is carbonic acid, HCO_3^- is bicarbonate, and CO_3^{2-} is dissolved carbonate. DIC accounts for 95% of the total marine carbon, and it is the sum of the following dissolved species:

$$DIC = CO_{2\,(d)} + H_2CO_3 + HCO_3^- + CO_3^{2-} \quad (3)$$

The physical and biological carbon pumps affect the storage capacity and the distribution of carbon in the oceans, including the distribution of DIC species. The physical pump is driven by the circulation pattern of the oceans, coupled with the existing temperature gradient that exists between low and northern high latitude waters (Rost et al., 2003; Killops and Killops, 2005; van Breugel, 2006). As the water moves toward high latitudes, CO_2 solubility increases. Based on how inorganic carbon is employed by organisms, the biological pump is divided into the organic pump and carbonate pump. The organic pump involves both the photosynthetic conversion of $CO_{2\,(d)}$ into biomass, which decreases marine DIC, and the subsequent transfer of this organic biomass to deeper waters and marine sediments (Figure 2). The transfer of organic carbon to deeper water involves the transformation of living biomass to particulate organic carbon (POC) upon the death of primary producers (Rost et al., 2003; Killops and Killops, 2005). POC is subsequently remineralized by microorganisms in intermediate to deep waters, which increases the DIC content in deep waters. The carbonate pump involves the transfer of calcium carbonate ($CaCO_3$) to deeper waters, which is precipitated by calcareous organisms in surface waters. This carbonate generation depletes surface waters in both Ca^{2+} and HCO_3^-. As this biogenic calcium carbonate reaches more acid waters at depth, dissolution could take place, producing DIC.

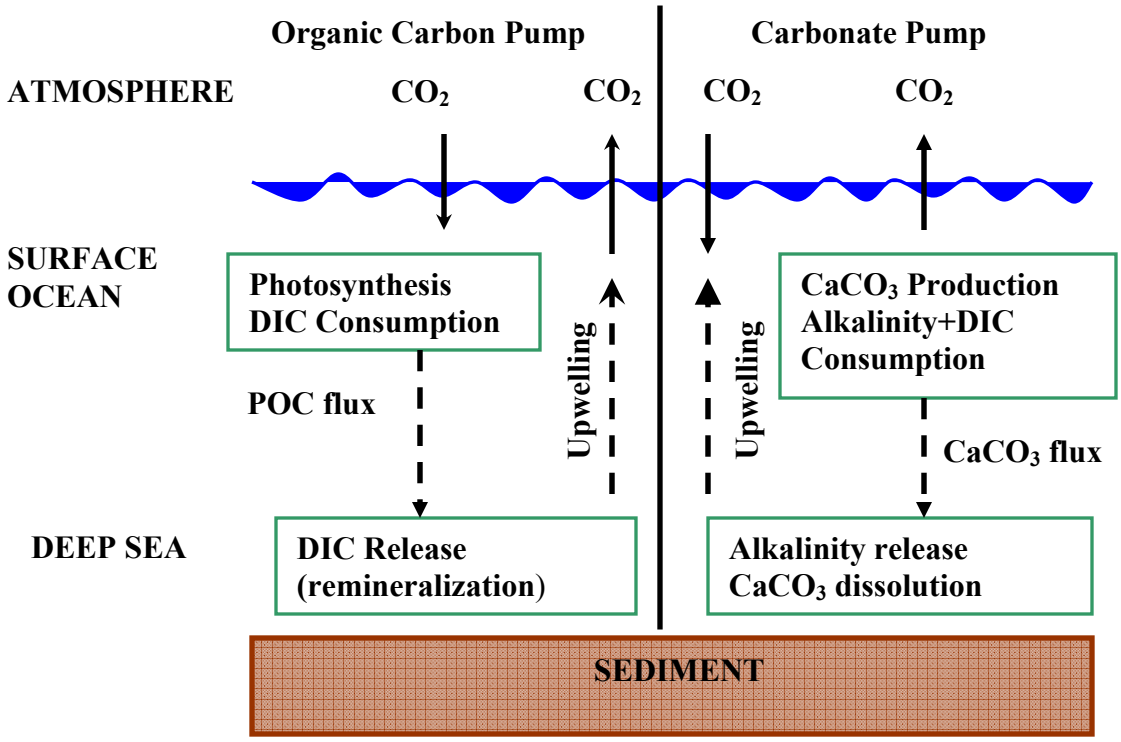

Figure 2. Biologic pumps (modified from Rost, 2003). Downward carbonate and particulate organic carbon flux contrasts with the upward flux of DIC and alkalinity.

DIC are generated in deep waters, thus producing a gradient in carbon concentration with depth (carbon-poor surface waters and carbon-rich deep waters). The carbonate pump transfers about 50 times more carbon (39,000 Gt) than the organic pump (730 Gt) (Figure 3). This release of DIC in deep waters makes the biological pump the most important agent influencing the vertical flux of DIC values and carbon inside the oceans. Consequently, any perturbation of these carbon pumps will produce changes in concentration and isotopic composition of the oceans from surface to depth waters. Ultimately, the isotopic signature associated with the process responsible for the perturbation will be recorded in both carbonates and sedimentary organic matter.

1.2. CARBON ISOTOPES FRACTIONATION

Isotopes are atoms of the same element with the same number of protons and electrons but different number of neutrons. Carbon has two stable isotopes, ^{12}C and ^{13}C. The two isotopes are unevenly distributed due to differential partitioning of isotopes (or fractionation) in carbon-bearing compounds during biotic (e.g., photosynthesis, microbial activity) and abiotic processes (e.g., precipitation, dissolution, weathering, etc.). As a result, the differential fractionation between stable isotopes of carbon can be used to monitor both ancient and current carbon-transfer processes, which affects the size of the different reservoirs inside the carbon cycle.

1.2.1. ISOTOPIC COMPOSITION OF DIC AND MASS BALANCE

The carbon-isotopic composition of DIC can be determined on the basis of the isotope mass balance that exists between the different dissolved species:

$$\delta^{13}C_{DIC} * DIC = \delta^{13}C_{CO2\,(d)} * CO_{2\,(d)} + \delta^{13}C_{H2CO3} * H_2CO_3 + \delta^{13}C_{HCO3^-} * HCO_3^- + \delta^{13}C_{CO3\,2-} * CO_3^{2-} \quad \textbf{(4)}$$

Equation 4 shows that marine biomass and carbonate formation/precipitation reflect the carbon isotope abundances of DIC and that both isotopic composition and concentration are directly proportional.

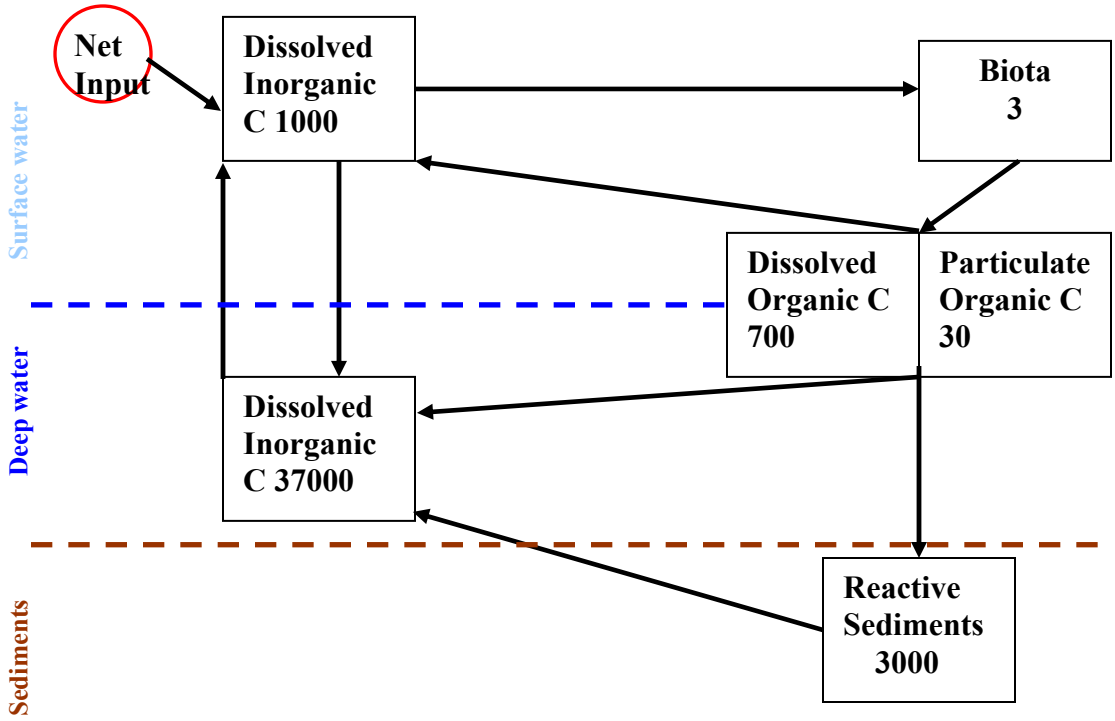

Figure 3. Marine carbon cycle showing sizes of reservoirs in Gt (boxes) and sources (arrows) (modified from Killops and Killops, 2005).

Therefore, any change in marine DIC concentrations could theoretically be detected from $\delta^{13}C$ values of marine sediments. For instance, the -4‰ excursion reported by Thomas et al. (2002) at the Paleocene-Eocene boundary (55 M.a.) affected the carbon pumps by introducing large amounts of methane into the atmosphere in a relatively short time period (~2 M.y.). This abrupt transfer of carbon with an extremely negative isotopic signature (-40‰) produced changes in carbon pumps functioning. Weissert et al. (1998) report three significant positive and one negative excursion in $\delta^{13}C_{carbonate}$ values during the Aptian (121-112 Ma). The positive $\delta^{13}C$ excursions are associated with a possible increase in carbon burial rates associated with oceanic anoxic events (OAE) (Jenkyns, 2003). During OAEs oxidation of organic matter is reduced, thus increasing marine carbon burial and preservation. This increasing burial modifies the carbon isotopic composition of the oceans.

Surface carbonates and organic matter are preserved in larger amounts, producing higher isotopic values (^{13}C-enriched). The negative excursion identified by Weissert et al. (1998) during the Early Aptian has been interpreted as to be the result of an ancient greenhouse event associated with the dissociation of large amounts (3000 Gt) of methane hydrates (Beerling et al., 2002).

Because of the size of the carbon pool in the oceans, only changes in the dynamics of the carbon pumps occurring throughout geologic time scales (long-term cycle) could shift the isotopic composition of DIC and, thus, marine carbonates. Once the isotopic composition of DIC has shifted, the carbon pumps exchange CO_2 with the atmosphere over short-term scales, thus modifying the isotopic composition of atmospheric CO_2 as well. Because the atmosphere is also in continuous interaction with the terrestrial biomass via photosynthesis, these changes in carbon isotopic compositions should also be transferred to plant biomass.

1.2.2. BIOLOGICALLY-MEDIATED FRACTIONATION OF CARBON ISOTOPES

During photosynthesis, primary producers uptake carbon from the CO_2 in the atmosphere or from the CO_2 dissolved in water. During the fixation process, these organisms preferentially include the lighter carbon isotope (^{12}C) into their biomass. There are two main types of photosynthetic pathways and, thus, two types of biologically-mediated isotope fractionation processes (Farquhar et al., 1989). While the vast majority of plants employ the Calvin cycle, and they are called C_3 plants, some grasses employ the Hatch-Slack cycle, the called C_4 plants (Galimov, 1985).

In C_3 organisms the process occurs in two steps. The first step is the diffusion of atmospheric CO_2 to the assimilatory centers. The fractionation in this step occurs when the CO_2 diffuses through air and into the cytoplasm (-4.4‰) of vascular plants (Galimov, 1985; Farquhar et al., 1989; Beerling, 1997; Hayes, 2001). Fractionation in the second step is significantly larger than in the first step (~ -29‰), and it occurs when the enzyme RUBISCO preferentially uses ^{12}C instead of ^{13}C to synthesize a three-carbon compound (enzymatic carboxylation, Figure 4).

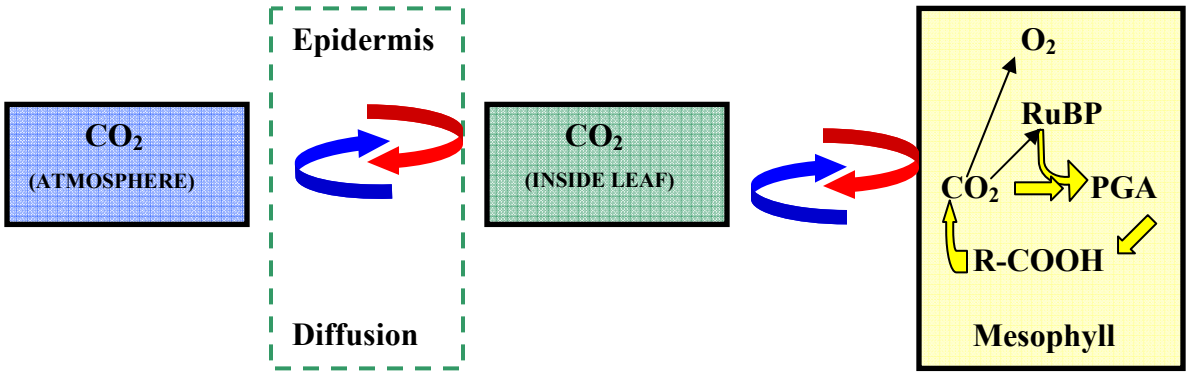

Figure 4. Isotopic discrimination during photosynthesis in vascular plants (modified from Schidlowski, 2001). The largest fractionation occurs inside the mesophyll (enzymatic carboxylation).

C_4 grasses discriminate less against ^{13}C than C_3 plants (Farquhar et al., 1989). Instead of the kinetic reaction with RUBISCO (-29‰) that performs most of the fractionation, photosynthesis in C_4 organisms includes an additional step. Before carbon reaches the mesophyll, it is used to produce oxaloacetate, a four-carbon compound synthesized by the enzyme phosphoenolpyruvate (PEP) carboxylase.

This enzyme discriminates less efficiently against ^{13}C (-5.7‰), and this reduced isotope discrimination effect results in higher carbon isotope values of plant biomass. Farquhar et al. (1989) proposed a model to explain the $\delta^{13}C$ values of photosynthetic organisms employing these two distinctive photosynthetic pathways. For plants following the Calvin cycle:

$$\delta^{13}C_{C3} = \delta^{13}C_{CO2} + a + (b-a)*(Ci / Ca) \qquad (5)$$

Where a is the fractionation that occurs due to diffusion through air (- 4.4 ‰), b is the fractionation caused by the carboxylation reaction (RUBISCO), Ci and Ca are the atmospheric and intracellular concentrations of CO_2, respectively. For C_4 organisms:

$$\delta^{13}C_{C4} = \delta^{13}C_{CO2} + a + (b_4 + b_3\Phi - a)*(Ci / Ca) \qquad (6)$$

.

Where b_4 is the effective discrimination of PEP carboxylase, b_3 is the discrimination due to RUBISCO, and Φ is the proportion of carbon that escapes from the Bundle sheath after the fixation process. Because the C_i/C_a ratio is the only variable in equations 5 and 6 for a given time interval, it largely determines the variability of $\delta^{13}C_{plant}$ values. Modern C4 plants exhibit an average $\delta^{13}C_{plant}$ value of -12‰, while modern standing C_3 plants have an average $\delta^{13}C_{plant}$ value that is about 20‰ depleted compared to the average atmospheric $\delta^{13}C_{CO2}$ value (O'Leary, 1988; Farquhar et al., 1989).

1.3. ISOTOPIC COMPOSITION OF SEDIMENTARY ORGANIC MATTER

1.3.1. $\delta^{13}C_{plant}$ VALUES AND BIOSYNTHESIS

The $\delta^{13}C$ values associated with land plant-derived organic matter present in rocks and sediments ($\delta^{13}C_{bulk}$) represents the average isotopic composition of plants ($\delta^{13}C_{plant}$), which is the average of the $\delta^{13}C$ values of the plant components preferentially preserved in the sediments (Arens and Jahren, 2000). Because of chemical and microbial alteration affecting terrestrial organic matter during the process of rock formation (diagenesis), some organic compounds are preferentially lost or degraded (Gröcke, 2002). Therefore, $\delta^{13}C_{bulk}$ values depend strongly on the isotopic composition of the organic components that are preferentially preserved. The carbon isotopic composition of these compounds varies as a result of the different isotope fractionation effects occurring during biosynthesis. Lipids, for instance, have more negative $\delta^{13}C$ values with respect to the whole plant values (Galimov, 1985; Hayes, 2001), which is significant considering that lipids are also one of the most resistant components to diagenetic processes (Figure 5). During diagenesis, bacteria preferentially metabolize ^{12}C from the sedimentary substrate, thus depleting the remaining organic matter in ^{12}C (Hartgers et al., 1994). Unlike lipids, nucleic acids, carbohydrates, and proteins exhibit less negative ^{13}C values than whole plant values, varying by less than 1‰ (Galimov, 1985; Hayes, 2001). The variability in isotope values among different organic constituents, their relative abundance, and their resistance to degradation determine the resultant carbon isotopic composition of sedimentary organic matter ($\delta^{13}C_{bulk}$).

If the parts preferentially preserved were, for example, seed-related compounds, which contain lipids, then the $\delta^{13}C_{bulk}$ value would be lower relative to $\delta^{13}C_{plant}$ values. On the other hand, if wood were preserved, the $\delta^{13}C$ value would be higher.

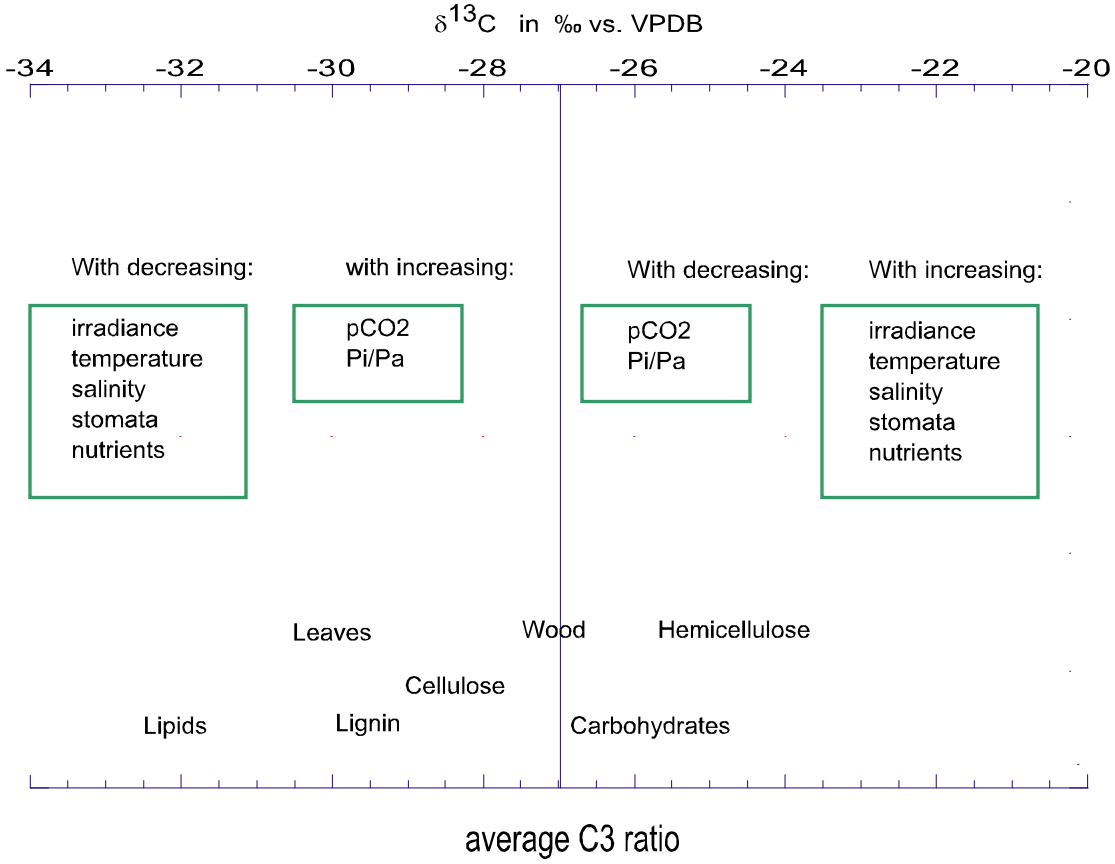

Figure 5. The effect of different environmental effects on the bulk isotopic composition of plant-derived organic matter (modified after Gröcke, 2002). The average $\delta^{13}C$ value for pre-industrial C_3 plants is around -27‰ as shown in the graph. Also note the difference in isotopic composition between plant components.

1.3.2. ENVIRONMENTAL STRESS

Light, water availability, salinity, atmospheric CO_2 concentration, and CO_2 recycling within the canopy are considered the primary environmental parameters affecting the carbon isotopic composition of vascular plants (Farquhar et al., 1989; Gröcke, 1998) (Figure 5), because they influence the Ci/Ca ratio (Equation 5).

Light influences the isotopic composition of the plant by determining the extent of stomata closure, which affects Ci (Equation 5) and thus $\delta^{13}C_{plant}$ values (Galimov, 1985; Farquhar et al., 1989). The lack of water in the soil shifts the isotopic composition of the plant to more positive values as a consequence of the stomata reduction (Beerling, 1997; Glumac et al., 1998; Gröcke, 1998; Beerling and Royer, 2002). The same effect is produced by an increase in salinity and canopy or atmospheric CO_2 concentration. Altitude, on the other hand, is the only stressor that produces a negative shift in the $\delta^{13}C$ value of the organism. With increasing altitude, the Ca diminishes and thus the ratio C_i/C_a increases, producing consequently a shift to more negative values.

1.4. $\delta^{13}C_{CO2}$ VALUES

Equation 5 proposes a quantitative relationship between the carbon isotopic composition of atmospheric CO_2 and land plants via photosynthesis. As a result, this equation has been used in several studies to infer changes in $\delta^{13}C_{CO2}$ values through the geologic past from changes in $\delta^{13}C_{bulk}$ values of terrestrial sequences (e.g., Bocherens et al., 1993; Stern at al., 1994; Sinha and Stott, 1994; Ghosh et al., 1995; Hasegawa et al. 1997; Beerling and Jolley, 1998; Arinobu et al., 1999; Gröcke et al., 1999; Utescher et al., 2000; Beerling et al., 2001; Ando et al., 2002; Jia et al., 2003; Strauss and Peters-Kottig, 2003; Hasegawa et al., 2003; Robinson and Hesselbo, 2004; Heimhofer et al., 2004; Harris et al., 2004; Magioncalda et al., 2004; Jahren et al., 2005).

The most common assumption behind the use of this approach includes that $\delta^{13}C_{bulk}$ values of sedimentary organic matter are identical to $\delta^{13}C_{plant}$ values. For instance, Arens et al. (2000) collected over 500 published measurements of $\delta^{13}C_{plant}$ values of vascular C_3 plants to illustrate that $\delta^{13}C_{CO2}$ values can be obtained from $\delta^{13}C_{plant}$ values. Relying on Farquhar et al. (1989) model and using a least-square regression of measured $\delta^{13}C_{CO2}$ and $\delta^{13}C_{plant}$ values, Arens et al. (2000) obtained the following relationship:

$$\delta^{13}C_{CO2} = (\delta^{13}C_{plant} + 1867)/1.10 \qquad (7)$$

Based on the results of the equation 7, Arens and Jahren (2000) suggest that $\delta^{13}C_{bulk}$ faithfully records $\delta^{13}C_{plant}$, allowing the substitution of $\delta^{13}C_{plant}$ by $\delta^{13}C_{bulk}$ in equation 7. Because of the connection between atmospheric CO_2 and marine DIC, then $\delta^{13}C_{bulk}$ values should reflect changes in $\delta^{13}C_{carbonate}$ values when applying equation 7. However, this assumed isotopic link between $\delta^{13}C_{bulk}$ and $\delta^{13}C_{carbonate}$ via $\delta^{13}C_{CO2}$, has not been fully tested. The goal of the present study is then to verify the proposed correlation between $\delta^{13}C_{bulk}$ values in terrestrial deposits and $\delta^{13}C_{carbonate}$ values; therefore, a terrestrial sequence accumulated during a time interval characterized by fairly large secular changes in $\delta^{13}C_{carbonate}$ values is needed. The sequence selected for this study covers the 65-50 M.a. time period, when secular changes in $\delta^{13}C_{carbonate}$ values have been identified (Zachos et al, 2001). In this study, the Paleocene-Eocene marine carbon-isotope record is compared to that of a terrestrial sequence from the South American tropics.

The Paleocene and Early Eocene epoch is a time characterized by increasing global warmth and reduced latitudinal temperature gradients compared with present day. Estimated mean annual global sea surface temperature increased from 8 to 14°C (Zachos et al., 2001). During this time interval, several isotopic anomalies have been reported in marine sequences from around the world (Hayes et al., 1999; Norris et al., 2001; Zachos et al., 2001; Hollis et al., 2005). During the early Paleocene (65-61 M.a.), $\delta^{13}C$ values recorded in marine sequences ($\delta^{13}C_{carbonate}$) decreased from 1.5‰ to 0.5‰ (Figure 6). This shift is commonly associated with the recovery of primary production after the Cretaceous-Tertiary extinction event. A positive shift is present in the late Paleocene, with values increasing from 0.5‰ to 2.5‰. This event appears to be related to the burial of large amounts of organic matter (Corfield and Norris, 1998). The third excursion is found at the Paleocene-Eocene boundary, recording a major negative excursion in $\delta^{13}C_{carbonate}$ values. This excursion has been related to the rapid release of large amounts of methane from marine hydrates ($1.12x10^3$ Gt) as estimated by several studies (Corfield and Norris, 1998; Bains et al., 1999; Zachos et al., 2001; Katz et al., 2001; Thomas et al., 2002; Sloan, 2003). Methane has extremely negative isotopic signature (~-60‰) and a rapid release of large amounts of methane can rapidly shift $\delta^{13}C_{carbonate}$ values (Thomas et al., 2002). A fourth shift occurred in the early Eocene, with values changing from 2.5‰ to -0.5‰. The shift reflects an extreme greenhouse climate, associated with the possible dissociation of methane but in less quantity relative to the one released at the Paleocene-Eocene boundary (Zachos et al., 1994; Corfield and Norris, 1998; Pearson and Palmer, 2000; Zachos et al., 2001; Thomas et al, 2002).

This negative shift in $\delta^{13}C_{carbonate}$ values coincides with a period of increasing sea-surface temperatures (from 8 to 12°C) known as the early Eocene climatic optimum (Corfield and Norris, 1998; Zachos et al., 2001). This last negative shift appears to be the result of the extinction of numerous benthic foraminifera taxa (^{13}C-depleted) that was caused by changes in the temperature gradient with depth in the oceans (Corfield and Norris, 1998).

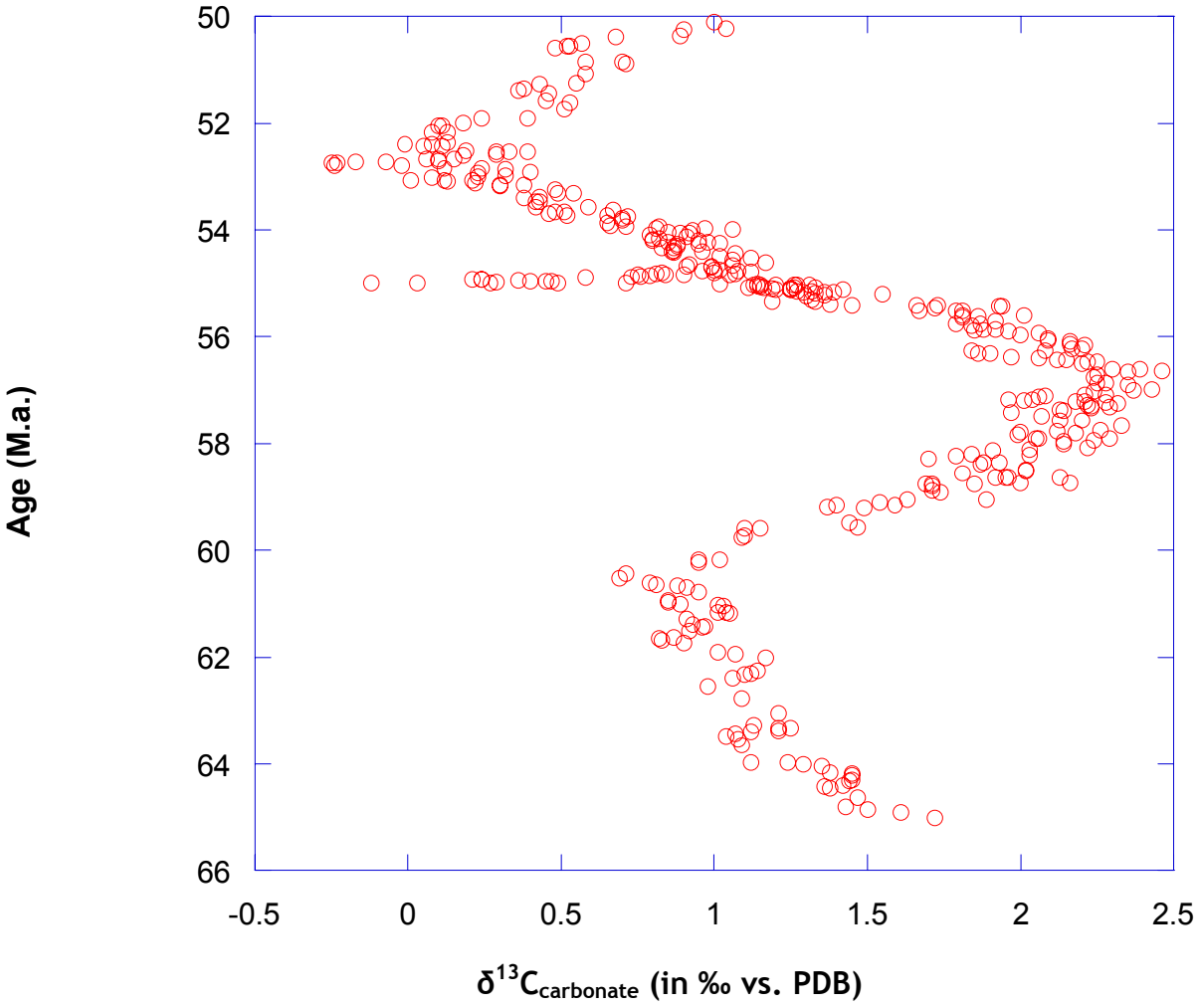

Figure 6. Global deep-sea carbon isotope records from 65 to 50 M.a. (modified after Zachos et al., 2001). The lithologies are predominantly fine-grained, carbonate-rich (50%) oozes or chalks.

The hypothesis postulated in this study predicts that the $\delta^{13}C_{bulk}$ values are expected to parallel the isotopic shifts shown in the $\delta^{13}C_{carbonate}$ values of Figure 6. However, factors such as diagenesis and depositional environment ultimately modify $\delta^{13}C_{bulk}$ values, thus compromising the use of $\delta^{13}C_{bulk}$ as a reliable correlation tool. The effects of diagenesis over $\delta^{13}C_{bulk}$ are not considered by Arens et al. (equation 7). During diagenesis, oxic bacteria preferentially metabolize ^{12}C-enriched organic matter, potentially enriching the remaining organic compounds in ^{13}C and possibly making $\delta^{13}C_{bulk}$ values more positive relative to $\delta^{13}C_{plant}$ values (Hartgers et al., 1994; Bergen and Poole, 2002). In addition, the depositional environment where the plant-derived organic matter accumulates dictates the type of plant component that is likely to be preserved. For instance, depositional environments with high sediment input and transport rates, as well as high oxygenation, preferentially preserve organic matter consisting of more resistant chemical compounds (Arens and Jahren, 2000; Gröcke, 2002), such as lipids, sporopollenin, and chitin; which tend to have more negative $\delta^{13}C$ values with respect to whole $\delta^{13}C_{plant}$ values (Figures 5 and 7).

Several studies have proposed different ways to overcome the potential isotopic overprinting produced during diagenesis. For instance, Beerling and Royer (2002) have proposed the use of a stomatal index to calculate past CO_2 concentrations accurately and thus infer past changes in carbon fluxes to and from the atmosphere. Although accurate, the technique requires the finding of fossil leaves with good preservation, which is somewhat difficult to achieve in most terrestrial sequences.

In addition, the effect of diagenetic alteration of organic matter on $\delta^{13}C_{bulk}$ values can be evaluated through the use of geochemical biomarkers, which are employed in this study.

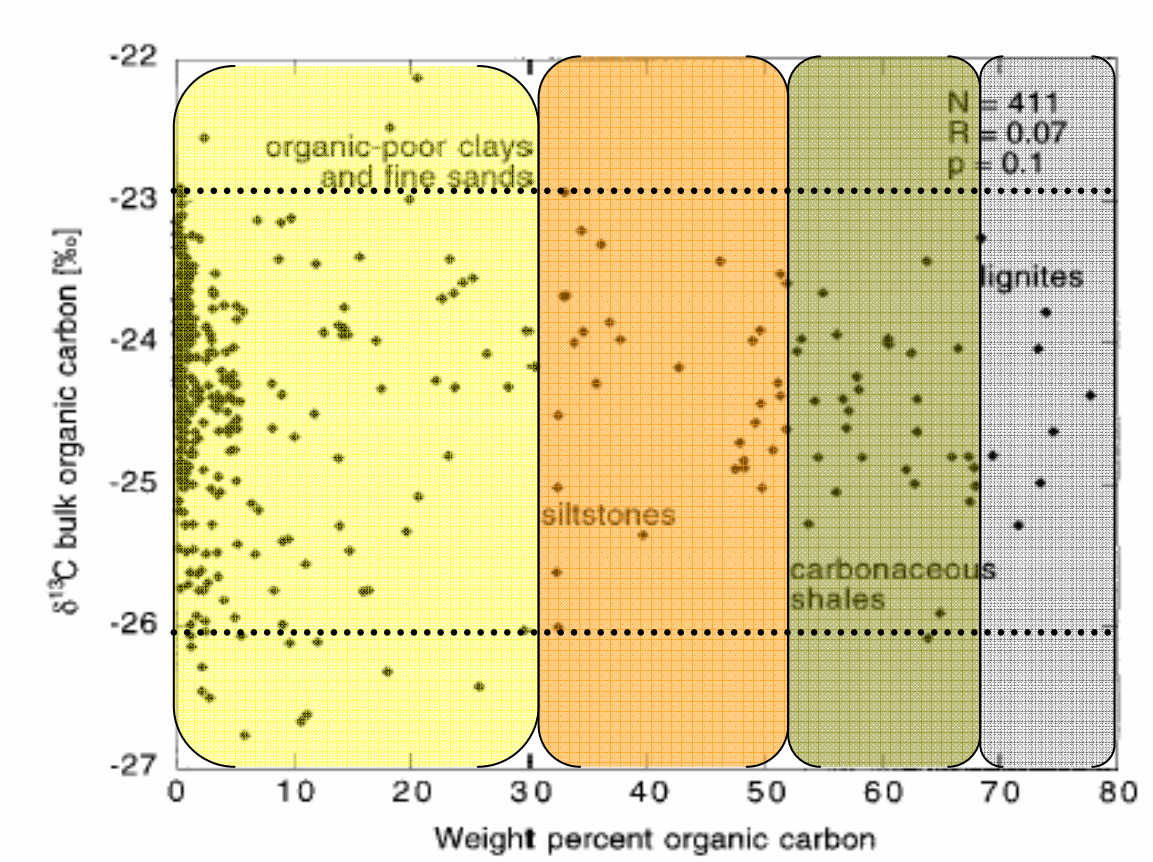

Figure 7. Variations in $\delta^{13}C_{bulk}$ values from samples covering the Cretaceous-Tertiary boundary (65 M.a.), as a function of the amount or carbon preserved in different depositional conditions (modified after Arens and Jahren, 2000). Peat-forming wetlands are characterized by a high preservation potential (grey and green zones), whereas well-drained flood plains offer poor preservation conditions for organic matter (yellow and orange zones).

Geochemical biomarkers are organic compounds that are found in rocks and sediments. These compounds possess carbon skeletons that are unambiguously linked to a known natural product.

Terrestrial plants, for example, produce characteristic biomarkers such us n-alkanes and terpenoids (e.g., (Otto et al., 2005), which allow their identification in the geologic record, and these two biomarker families are used in this study. Because different organisms synthesize different quantities and types of n-alkanes, these compounds are typically employed in studies evaluating the source of organic matter in sedimentary rocks (Otto et al., 2005). For instance, $nC_{27,}$ $nC_{29,}$ and nC_{31} n-alkanes have higher concentrations in land plant-derived organic matter relative to other n-alkanes. Terpenoids are other organic compounds synthesized by vascular plants (Peters et al., 2005), and they are formed from isoprene units, which create both acyclic (isoprenoids) and cyclic terpenoids (mono-, sesqui-, di-, tri-, tetra-, and penta-cyclic terpenoids).

In this study, a set of biomarker parameters is used to qualitatively evaluate microbial- versus plant-derived contributions to the organic matter present in a set of samples selected from a terrestrial sequence. These findings also allow an evaluation of the potential effect of microbial degradation on $\delta^{13}C_{bulk}$ values, thus making it possible to determine potential biases, which could undermine the use of $\delta^{13}C_{bulk}$ values as a reliable proxy for various geochemical studies.

1.5. GEOLOGICAL SETTING

During the late Cretaceous and Early Paleogene, tectonically-driven changes in depositional styles took place in northern South America by the reactivation of the Central cordillera uplift (Villamil, 1999), resulting in changes in depositional styles: from a marine-dominated to a terrestrial-dominated sedimentation setting. Characteristic depositional environments associated with these terrestrial settings included swamps, marshes, flood plains, and oxbow lakes. Sediments accumulated in those environments are part of the Catatumbo and lower Barco Formations (Villamil, 1999).

1.6. STUDY SITE

Figure 8 shows the location of the sample sites during the middle to late Paleocene and early Eocene. The samples for this study were collected from two well sites that are located at 8°12'N, 72°1'1"W (Gonzalez-1 well) and 9°34'16"N, 73°16'45"W (Diablito-1 well) (Figure 9). The Gonzalez-1 well is located within the Catatumbo basin, whereas the Diablito-1 well is located within the Cesar-Rancheria basin (Figure 9). Sampling was performed every 9.14 m in average on each well to cover the desired time span, yielding a set of 158 samples (72 from the Gonzalez-1 and 86 from the Diablito wells, respectively), which were chronostratigraphically constrained by fossil pollen (Figure 10) with an average time resolution of 0.1866 M.y./sample (maximum = 0.3925 M.y./sample; min = 0.0654 M.y./sample).

The sedimentation rates during the time interval were in average 41.36 m/M.y. and 41.437 m/M.y. for the Gonzalez-1 and Diablito-1 samples, respectively. These sampled sediments consist of mudstones, coals, and small lenses of sandstones probably accumulated in a transitional setting (Catatumbo and Barco Formations) and in a mixture of deltaic and fluvial conditions (Cuervos Formation).

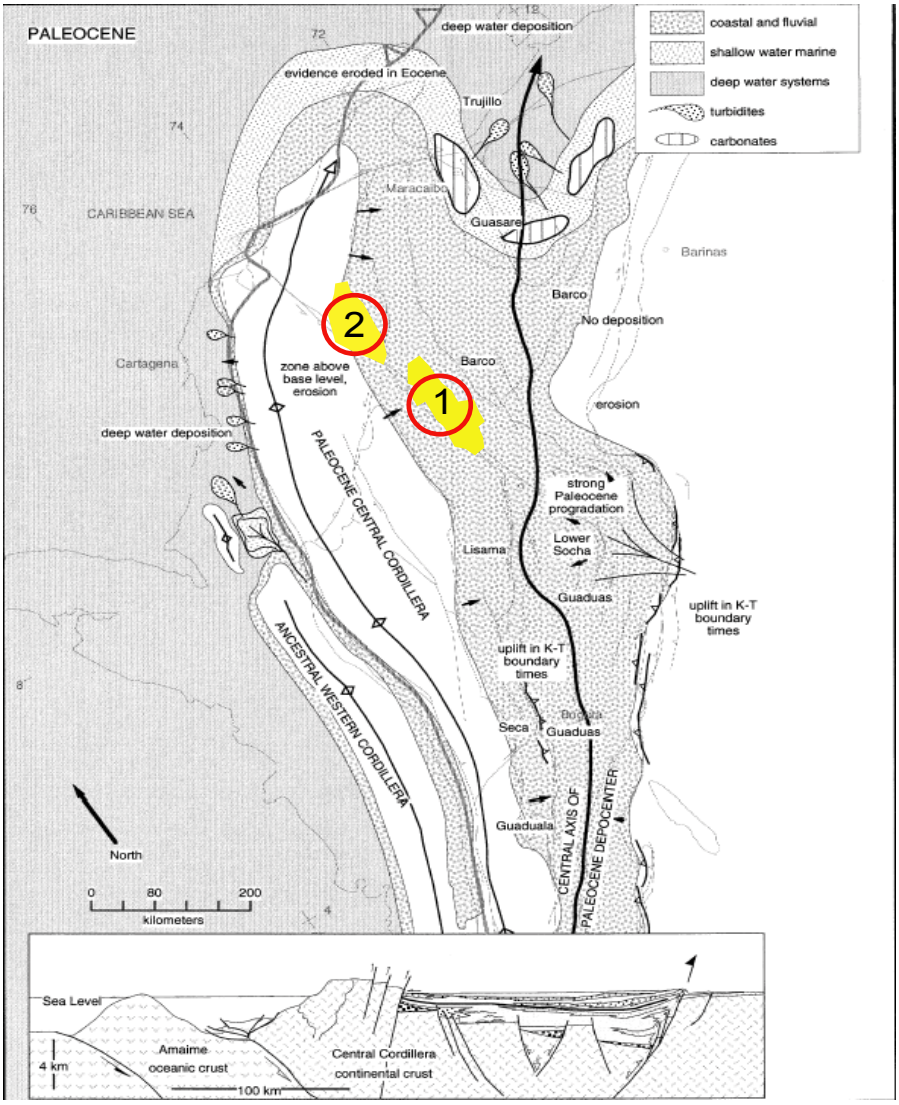

Figure 8. Facies map representing a marked decrease in accommodation space and infill of the marine seaway by coastal and deltaic deposits derived from the east and west (modified from Villamil, 1999). Catatumbo (1) and Cesar-Rancheria Basins (2) are highlighted in yellow.

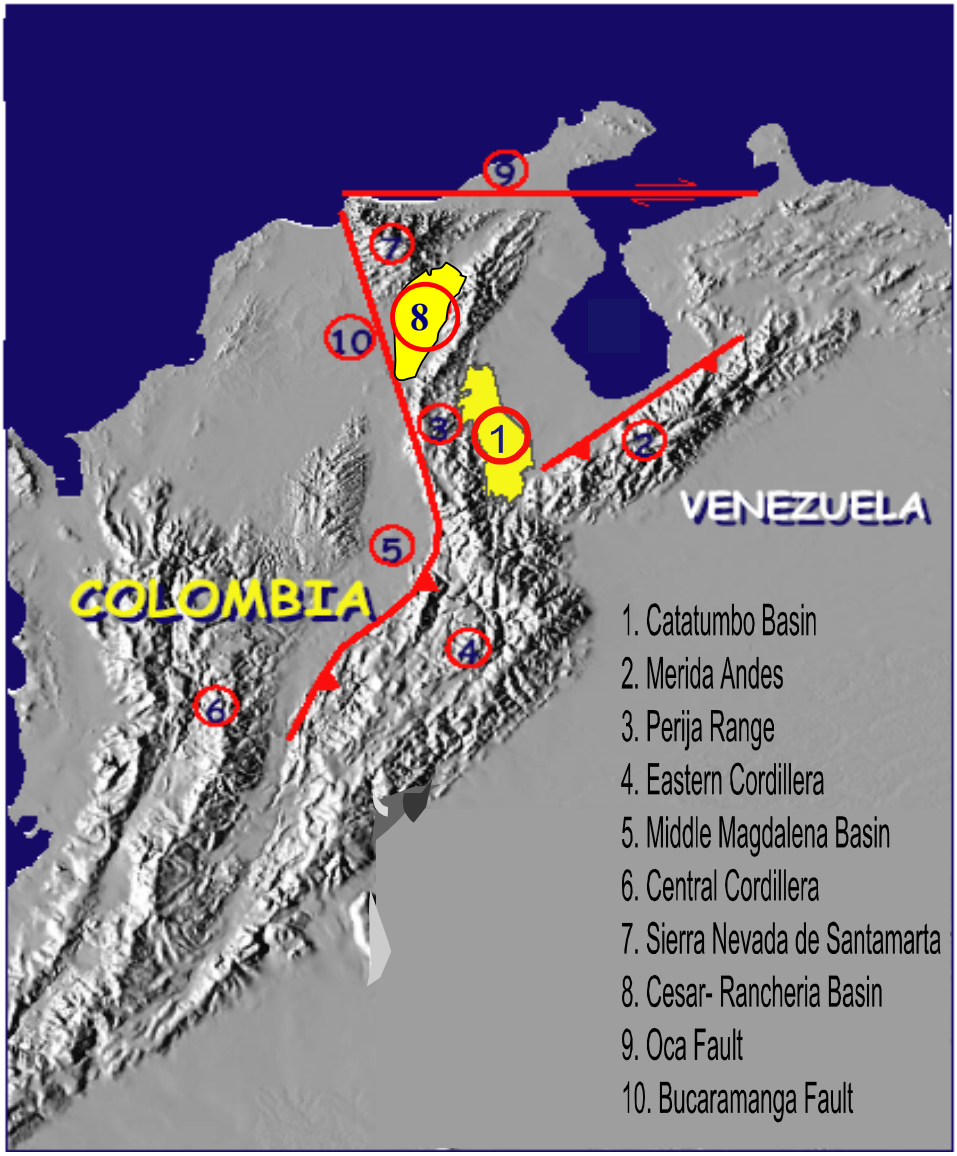

Figure 9. Map of northern South America, showing the most important tectonic features and sedimentary basins of northern Colombia and western Venezuela. The studied rocks came from well cuttings of the Gonzalez-1 and Diablito-1 wells (Catatumbo and Cesar-rancheria Basins, respectively).

2. ANALYTICAL METHODS

2.1. BULK SEDIMENT ISOTOPIC ANALYSIS

Stable carbon isotope analyses of bulk sediment ($\delta^{13}C_{bulk}$) were performed in the Department of Geological and Atmospheric sciences at Iowa State University. For $\delta^{13}C_{bulk}$ measurements, rock samples were air-dried and powdered with an agate pestle and mortar. Aliquots of 1-2 g of powdered rock sample were acidified with 1M hydrochloric acid overnight to remove carbonates. Samples were neutralized by repeatedly rinsing the decalcified sample with de-ionized/distilled water. Neutralized samples were then freeze-dried overnight. Aliquots of 30 to 90 mg of the residue were weighed out and analyzed for stable isotopes of carbon via pyrolisis at 1100^{o}C in a COSTECH elemental analyzer fitted to a Thermo Finnigan Delta ^{plus}XL isotope ratio mass spectrometer. Helium was used as a carrier gas to transport the liberated CO_2 from the elemental analyzer to the mass-spectrometer. Analytical precision and accuracy was determined on the basis of repeated analysis of two internal lab standards calibrated against the internationally accepted V-PDB standard. Overall uncertainty was better than 0.08 ‰. Organic carbon content was determined on the basis of the liberated CO_2 in the elemental analyzer. Overall uncertainty of the organic contents was better than 6% as determined by repeated measurements of internal lab standards. A five-point moving average was applied to the $\delta^{13}C_{bulk}$ values from both Diablito-1 and Gonzalez-1 wells to minimize sample-related noise.

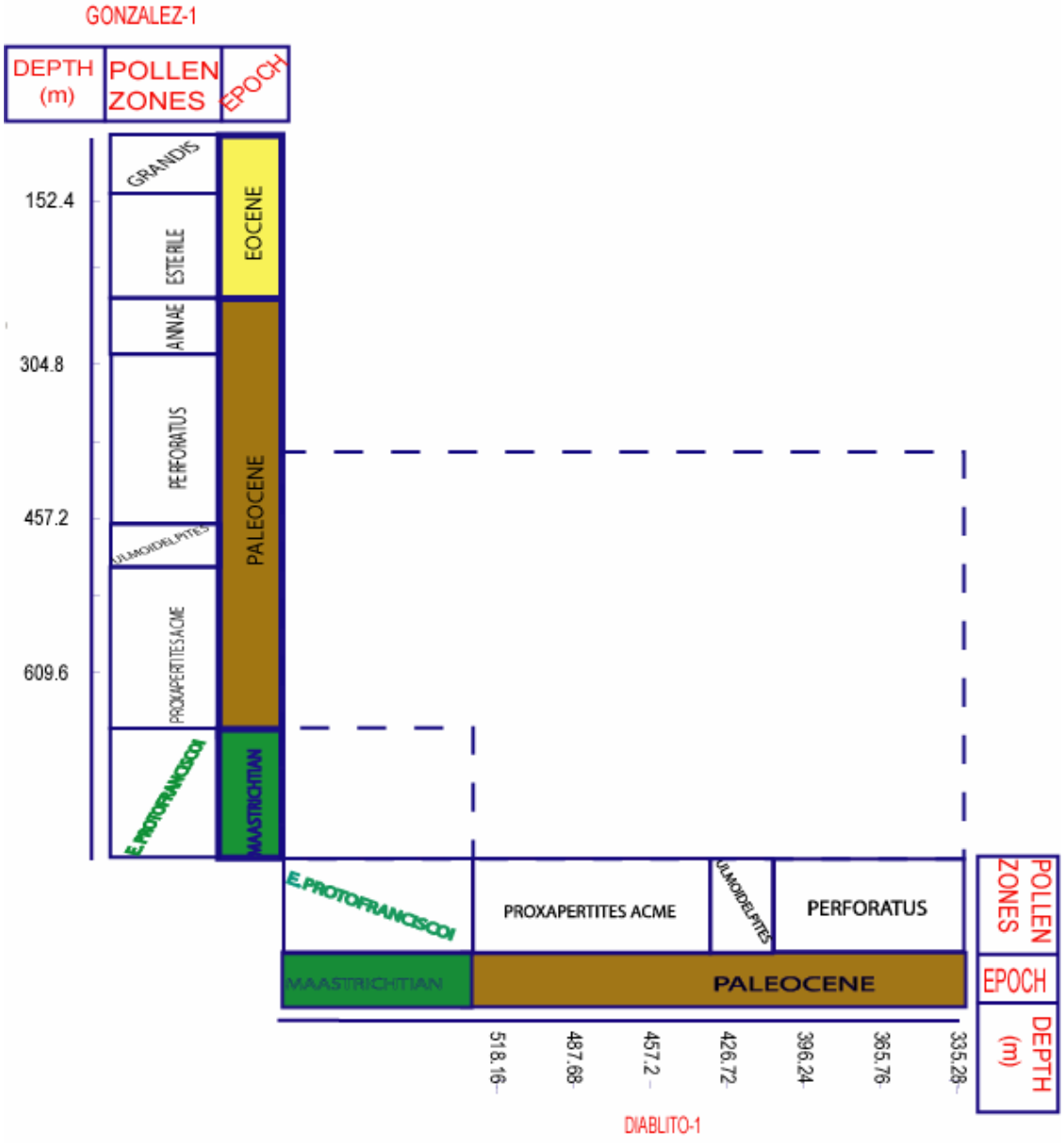

Figure 10. Chronostratigraphy for the Catatumbo and Cesar-Rancheria basins. The geologic ages are based on pollen zones developed for the area using samples from Gonzalez-1 and Diablito-1 wells.

2.2. BIOMARKER ANALYSIS

2.2.1. SOLUBLE ORGANIC MATTER EXTRACTION (SOM)

A set of 27 samples from the initial 158 were selected for biomarker analysis on the basis of their organic carbon content and on their relative stratigraphic location to represent the entire sequence. SOM extraction followed the methodology proposed by Otto et al. (2005). Five grams of ground, dried sediments were placed in cleaned, pre-combusted, 50 ml glass test tubes. The samples were sonicated six times for 10 minutes, each with a 250 ml solution of 6:1 dichloromethane/methanol. The extracted SOM was transferred into a 250 ml rounded flask through a separatory funnel containing a cellulose filter paper that captured sediment particles. Extracted SOM was concentrated using a Büchi Rotovapor R-200 at 50^{o}C and transferred to a 10ml vial. After completing volume with dichloromethane, a 1 ml aliquot of extracted SOM was placed in a pre-weighed 2 ml vial, refrigerated overnight to precipitate asphaltenes, and centrifuged to remove the precipitate from the solution. The solvent was evaporated from the solution using nitrogen gas and hexane was added to complete 1 ml. The saturated and aromatic fractions were separated using micro column chromatography and activated silica gel. The fractions were eluted with hexane and benzene, respectively. To allow for a better chromatographic separation, the aliphatic and aromatic fractions were derivatized with 100µL of N, O,-bis (trimethylsilyl) trifluoracetamide and trimethylchlorosilane (BSTFA/TMS 99:1) at 65°C for30 min.

2.2.2. GAS CHROMATOGRAPHY-MASS SPECTROMETRY

Gas chromatography–mass spectrometry (GC–MS) analyses of the derivatized samples were performed on an Agilent model 6890 GC coupled to a Micromass GC-TOF MS located at the Chemical Instrumentation Facility center of the Chemistry Department and an Agilent A 6890 N gas chromatograph/5973 network mass spectrometer located at the biogeochemistry lab of the Geological and Atmospheric Sciences Department at Iowa State University. Separation was achieved with a fused DB5 silica capillary column and with helium as the carrier gas. The GC operating temperature ramp was as follows: temperature was held at 65°C for 2 min, and then increased from 65 to 300°C at a rate of 6°C/min, with final isothermal hold at 300°C for 15 min. The sample was injected splitless with the injector temperature at 300°C. The mass spectrometer was operated in the electron impact mode (EI) at 70 eV ionization energy and scanned from 40 to 650 Dalton. Individual compounds were identified by comparison of their mass spectra and retention times with those of published compounds and by interpreting mass fragmentation patterns. Relative abundances of the different compounds were calculated using peak areas in the total ion current (TIC) of the derivatized total extracts. Some individual compounds were identified using the GC trace of a selected ion mass (SIM).

3. RESULTS

3.1. BULK GEOCHEMICAL PARAMETERS

3.1.1. TOTAL ORGANIC CARBON

Most of the samples analyzed are mudstones that vary in color from black or dark gray to slightly dark brown, typical for samples with relative high content of organic matter. Visible woody fragments were observed in some of the samples. Organic carbon contents (C_{org}) vary between 0.01 and 11.24 wt. % (Appendix 1 and Figure 11). The lowest carbon contents were found in the Barco Formation (0.96 wt. % in average), corresponding to depths between 460 and 350m in the Gonzalez-1 well, and the highest contents were found in samples from the Cuervos Formation (2.00 wt.% in average), corresponding to depths between 350 and 150m in the Gonzalez-1 well.

3.2. CARBON ISOTOPIC COMPOSITION OF ORGANIC MATTER

The $\delta^{13}C_{bulk}$ values for the Gonzalez-1 samples show three carbon-isotope excursions: a positive shift at 350 m and two negative shifts at 500 and 200 m (Figure 12). The $\delta^{13}C_{bulk}$ values for Diablito-1 samples range from 273 to 700 m.

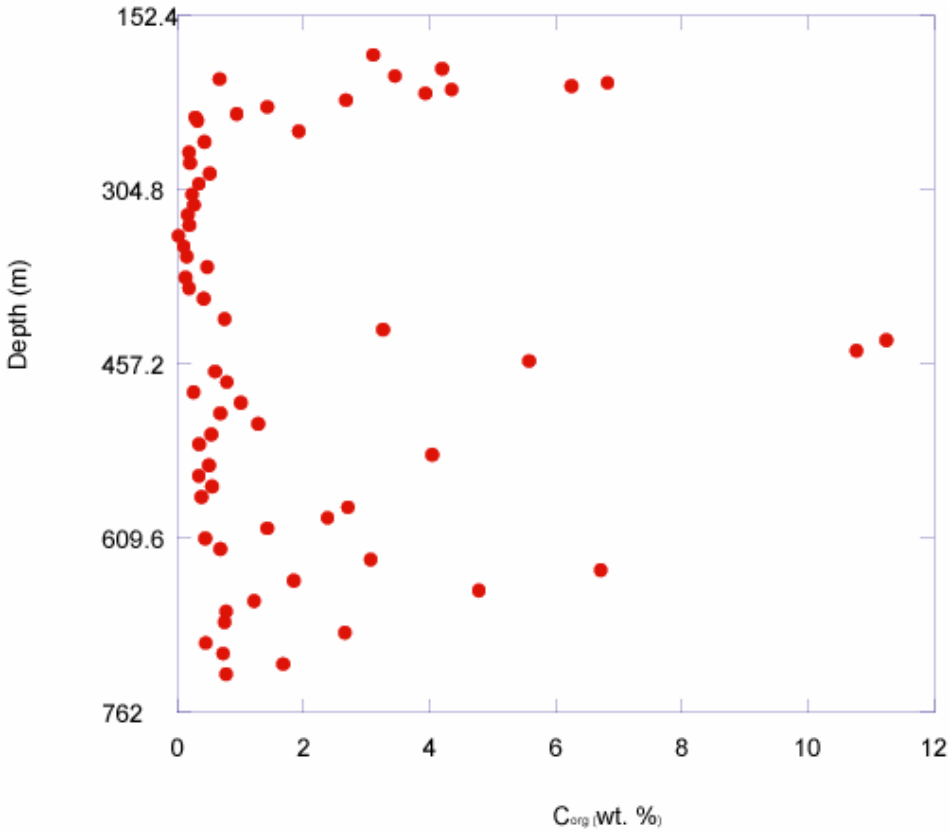

Figure 11. Total organic carbon content (C_{org}) in weight percentage for the Gonzalez-1 samples.

The three carbon-isotope excursions found in the Gonzalez-1 samples chronostratigraphically correlate with those found in marine carbonates (Zachos et al., 2001; Figure 12). The $\delta^{13}C_{bulk}$ values decrease from -24‰ to -26‰ from 65 to 58 M.a. This shift correlates with that in marine carbonates from 1.75‰ to 0.5‰ for the same interval. A positive shift in $\delta^{13}C_{bulk}$ values occurs in the late Paleocene (58-56 M.a.), with values becoming less negative from -26.5‰ to -23.8‰. In the marine record, this excursion is represented by a shift from 0.5‰ to 2.5‰. The third excursion occurs near the Paleocene-Eocene boundary (55 M.a.), with values

changing from -23.8‰ to -26.5‰ and from 2.5 to -0.25‰ in the terrestrial and marine records, respectively.

One aspect that is absent in the $\delta^{13}C_{bulk}$ record is the sharp spike in marine carbonate $\delta^{13}C$ values at the Paleocene-Eocene boundary (55 M.a.), which is known as the Paleocene-Eocene thermal maximum (Koch et al., 1992; Bralower et al., 1997; Dickens et al., 1997; Koch et al., 1998; Zachos et al., 2001). Its absence in the $\delta^{13}C_{bulk}$ data set is probably due to the large sampling intervals (0.2 M.y./sample) employed for this study and the short duration of this event.

3.3. ASPHALTENE ABUNDANCE

The organic extracts contained asphaltenes, aliphatics, aromatics, and NSO compounds. Asphaltenes were present in relative high abundances within each extract, averaging 16 mg/g C_{org} in both Diablito-1 and Gonzalez-1 samples (Appendix 1). Asphaltenes abundances in Diablito-1 samples are as low as 3.76 mg/g C_{org} (487-500m) and as high as 43.83 mg/g C_{org} (450-460m) (Figure 13). Asphaltene abundances in Gonzalez-1 samples vary from 1.06 mg/g C_{org} (152m) to 43.57 mg/g C_{org} (500m).

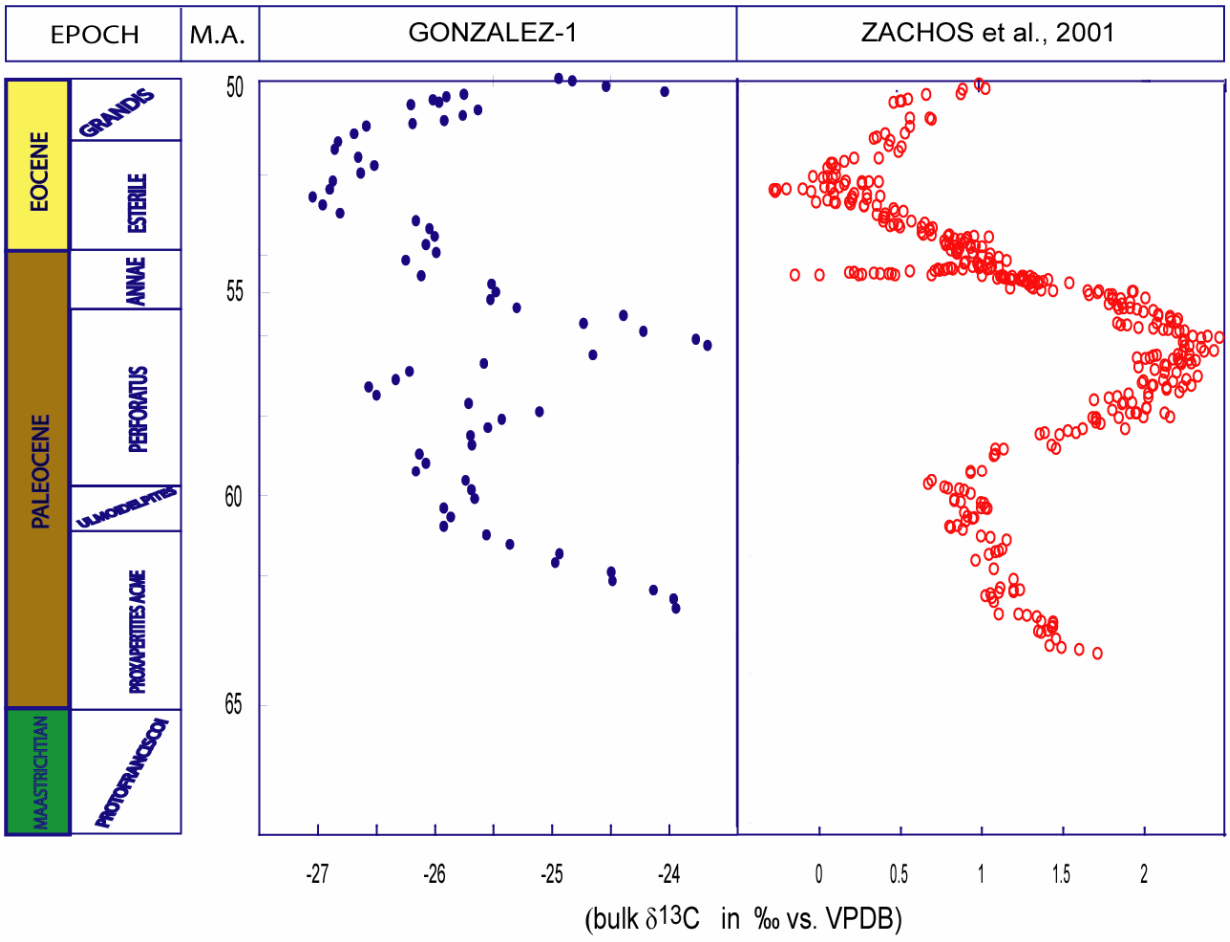

Figure 12. Comparison between the carbon isotopic composition of terrestrial organic matter (Gonzalez-1) and that of marine carbonates (from Zachos et al., 2001) during the Paleocene-early Eocene.

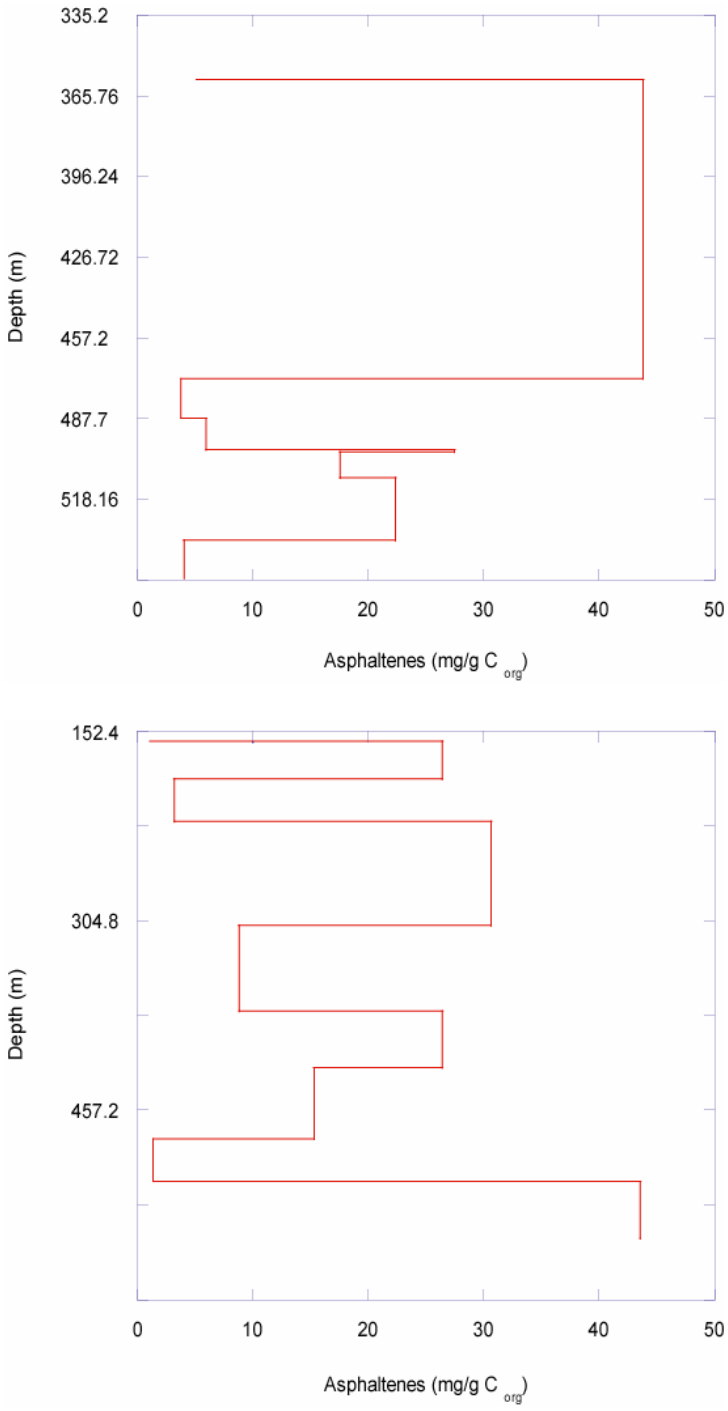

Figure 13. Asphaltenes distribution with depth in the Diablito-1 (upper panel) and Gonzalez-1 (lower panel) wells.

3.4. MOLECULAR COMPOSITION OF ORGANIC MATTER

Analyses of the aromatic fraction revealed the absence of compounds in significant abundances. Thus, this study reports the compounds identified in the aliphatic fraction of SOM. Four major families of organic compounds were identified in the aliphatic fraction: n-alkanes, regular acyclic isoprenoids, sesqui-and triterpenoids. Mid and short-chain n-alkanes, as well as triterpenoids are the most abundant types of compounds present in the studied samples (Figure14).

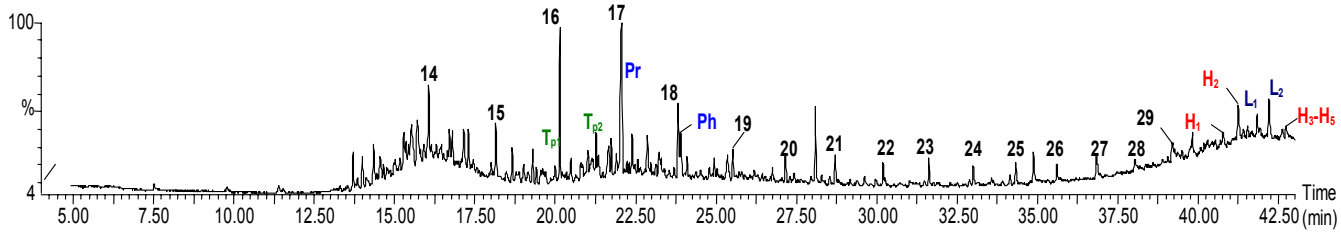

Figure 14. Common GC-trace displaying the retention times (X-axis) and the relative abundances (Y-axis) of the identified compounds. Peaks with bold black numbers correspond to n-alkanes. Isoprenoids, sesquiterpenoids, non-hopanoid triterpenoids, and hopanoids are shown in blue, green, dark blue, and red, respectively (see also Appendix 2).

3.4.1. n-ALKANES AND ISOPRENOIDS.

The n-alkane distribution in the studied samples shows an odd-over-even-predominance, with high abundances of short-chain n-alkanes (<nC_{20}) (Appendix 2 and Figure 15). The identified isoprenoids pristane (Pr) and phytane (Ph) are

present in most of the samples, with Pr typically being more abundant than Ph. (e.g., Figure 14 and Appendix 1). Because of their interdependent response to changes in the depositional environment, Didyk et al. (1978) proposed the use of the pristane/phytane ratio (Pr/Ph) as the a proxy for the level of oxicity in the sediments, with low Pr/Ph values (between 1.5 and 2.5) reflecting deposition under dysoxic conditions and high Pr/Ph values indicating deposition under oxic conditions. Diablito-1 Pr/Ph values vary between 0.81 and 2.79, with a decreasing trend with depth (Appendix 1). Gonzalez-1 Pr/Ph values range from 0.94 to 4.59 with no significant trend with depth (Appendix 1). These values suggest a changing level of oxygen in the sediments during the accumulation of the studied sequences. Overall oxygen levels also were evaluated through the Pr/nC_{17} vs. Ph/nC_{18} relationship (Peters et al., 2005). This index also suggests that the environment where the studied sediments accumulated experienced shifts from oxidizing to reducing conditions (Figure 16). The zones on Figure 16 represent the three main types or organic matter based on the ratio Oxygen/Carbon vs. Hydrogen/Carbon (Tissot and Welte, 1984): type I (lacustrine), type II (marine), and type III (terrestrial plants).

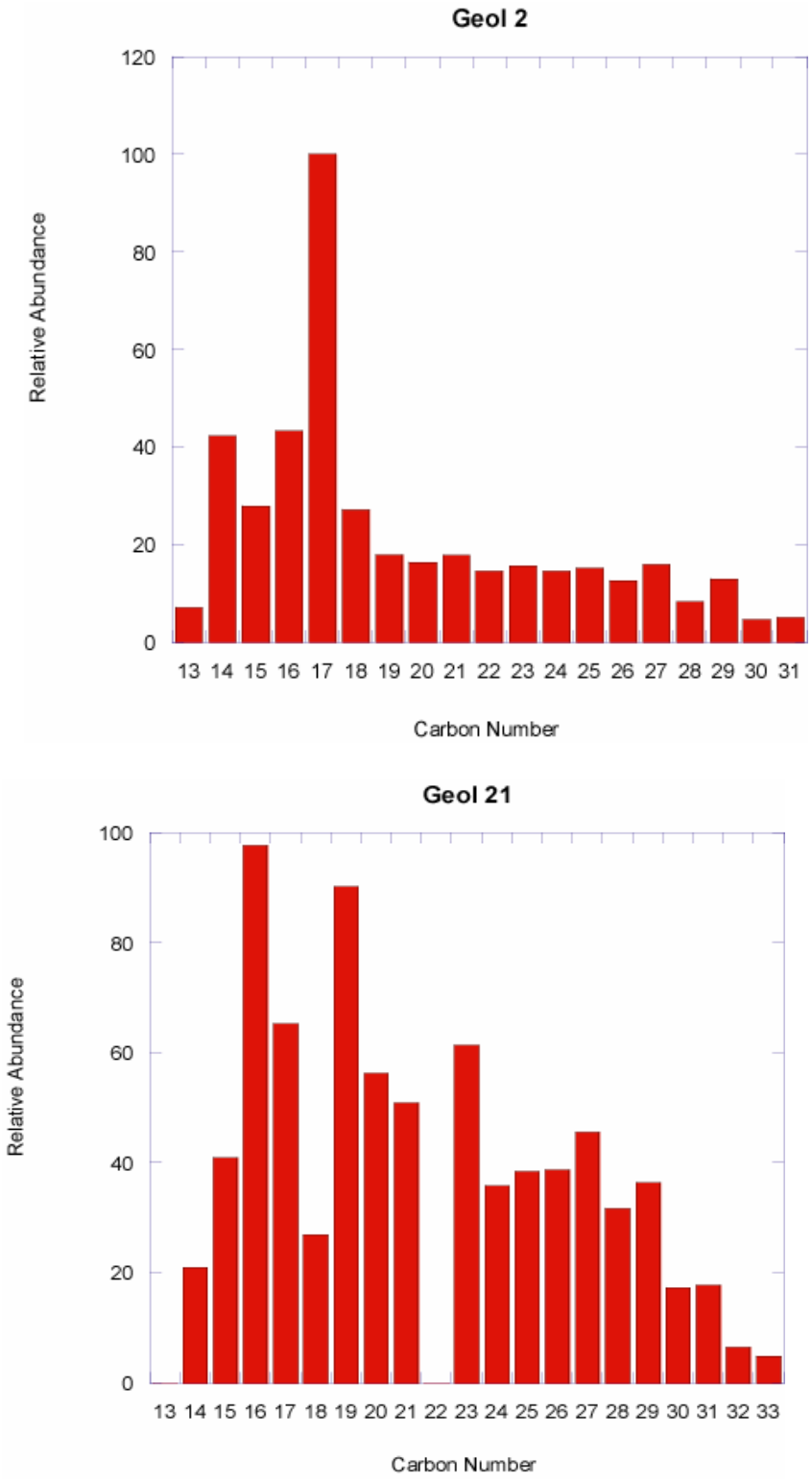

Figure 15. Histogram of the relative abundance of n-alkanes for the Diablito-1 (upper panel) and Gonzalez-1 (lower panel) samples.

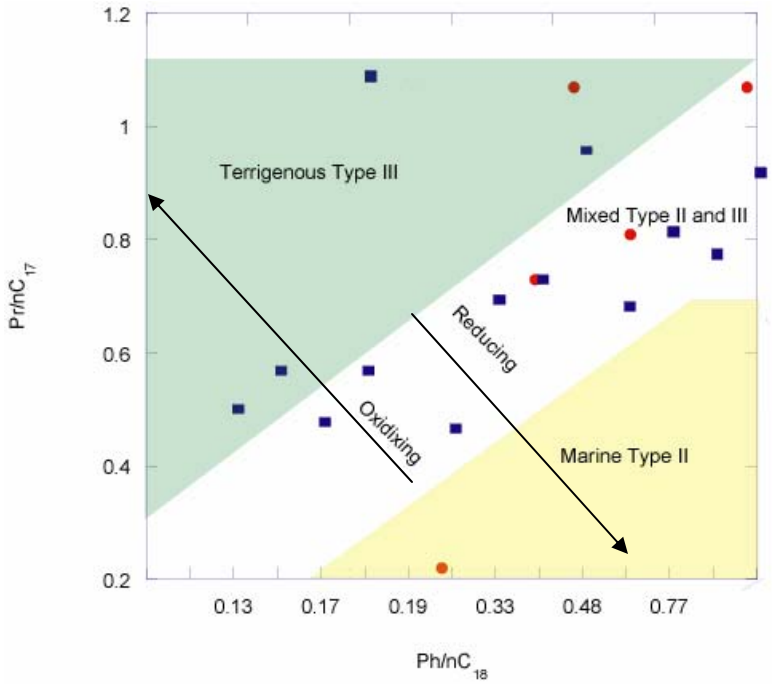

Figure 16. Pr/nC_{17} vs. Ph/nC_{18} showing levels of oxicity and organic matter type (after Peters et al., 2005) for Diablito-1 (red circles) and Gonzalez-1 (blue squares) samples.

3.4.2. SESQUITERPENOIDS AND NON-HOPANOID TRITERPENOIDS

Two types of sesquiterpenoids are present in the saturated fraction of the SOM: a C-16 sesquiterpenoid and a cadalene-type sesquiterpenoid. The identification of the two sesquiterpenoids was achieved by the presence of the characteristic fragments 183 and 123 in the mass spectra (Figure 17 and Appendix 2) and by comparisons to published spectra of these compounds (Philp, 1985; Otto et al., 1997; Otto and Simoneit, 2001; Bechtel et al., 2003; Hautevelle et al., 2006). The non-hopanoid triterpenoids identified in the saturated fraction correspond to lupane- and moretane-type triterpenoids (Figure 20).

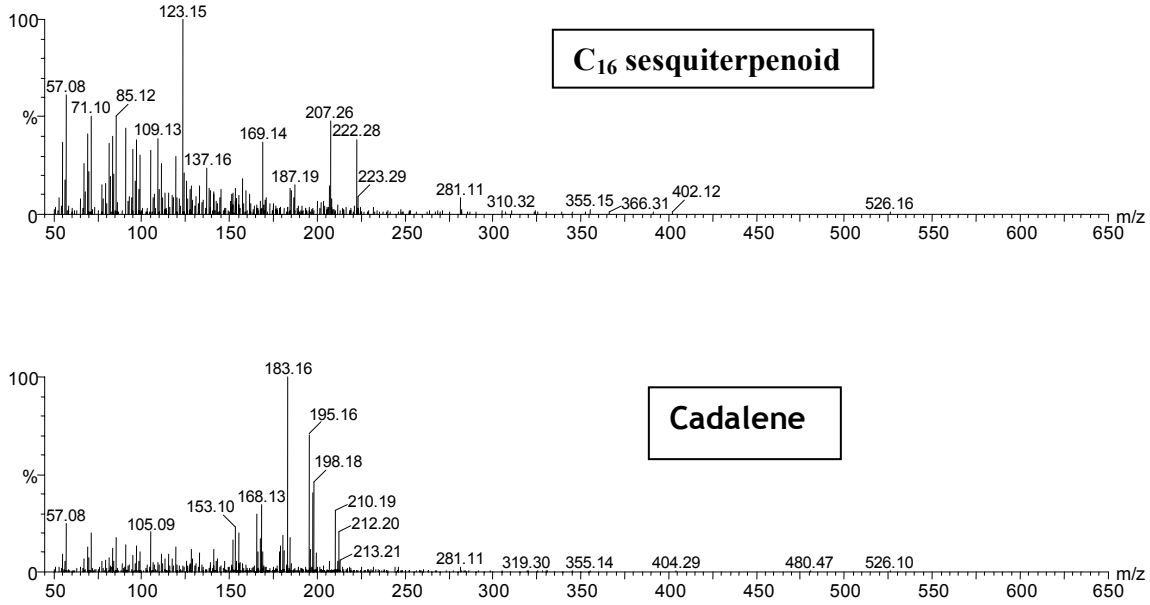

Figure 17. Mass spectra of the two sesquiterpenoids identified in the Gonzalez-1 and Diablito-1 samples: C_{16} sesquiterpenoid (upper panel) and a cadalene-type compound (lower panel).

3.4.3. HOPANOIDS

Hopanoids, after n-alkanes, are the main constituents present in the saturated fraction of both Diablito-1 and Gonzalez-1 samples (Appendix 2 and Figure 14). Hopanoids are compounds occurring in bacteria (Peters et al., 2005; Killops and Killops, 2005; Otto et al., 2005). The identified hopanoids compounds correspond to 17α-22,24,30-trisnorhopane, 17α(H),21β(H)-hopane, 17α,21β(H)-norhopane, 17β(H),21β(H)-hopane, 17α(H),21β(H)-homohopane, 17β(H),21β(H)-homohopane, unknown C_{32} hopanoid, and 17α(H),21β(H)-trishomohopane (H1,H2,H3,H4,H5,H6,H7,H8, respectively) (Appendix 2 and Figure 14). Both well samples display similar hopanoid distributions (Figure 19), although the heavier

hopanoids (H5 through H8) are commonly absent in the Diablito-1 samples (Appendix 2).

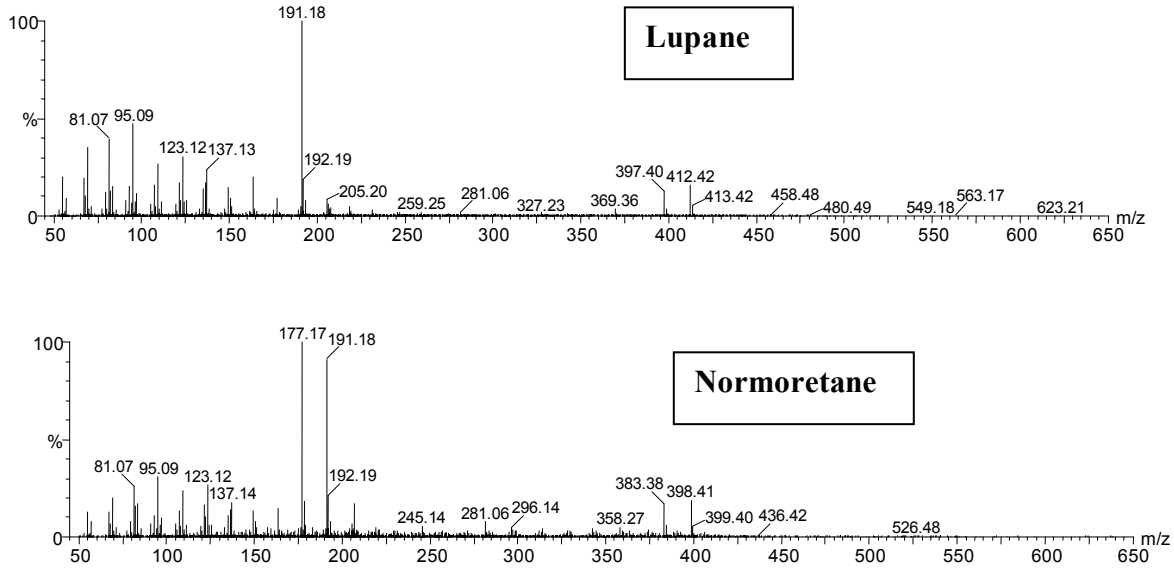

Figure 18. Mass spectra of the two non-hopanoid triterpenoids identified in the Gonzalez-1 and Diablito-1 samples: lupane (upper panel) and a normoretane-type compound (lower panel).

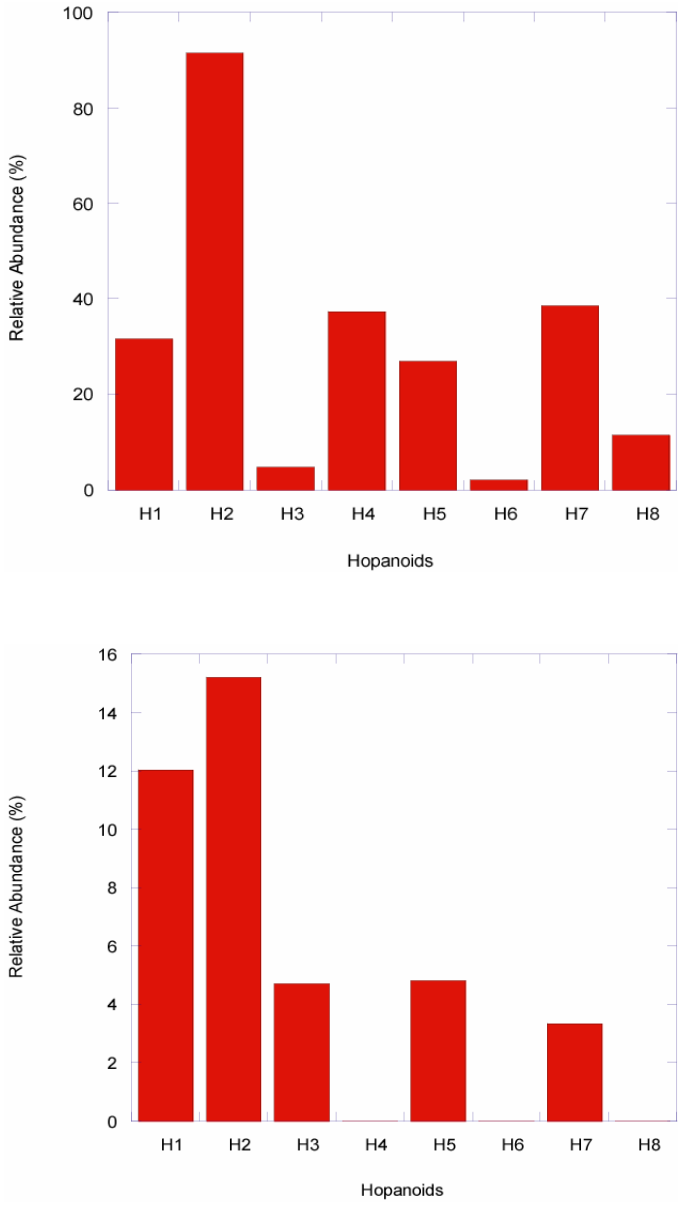

Figure 19. Histograms of the distribution patterns of hopanoids in the Diablito-1 (lower panel) and Gonzalez-1 (upper panel) samples. The identified hopanoids compounds correspond to 17α-22,24,30-trisnorhopane, 17α(H),21β(H)-hopane, 17α,21β(H)-norhopane, 17β(H),21β(H)-hopane, 17α(H),21β(H)-homohopane, 17β(H),21β(H)-homohopane, unknown C_{32} hopanoid, and 17α(H),21β(H)-trishomohopane (H1,H2,H3,H4,H5,H6,H7,H8, respectively).

4. DISCUSSION

4.1. THE $\delta^{13}C_{bulk}$ VALUES AS A PROXY FOR CHANGES IN THE CARBON CYCLE

The carbon isotopic composition of plant-derived organic matter has been used in geologic studies to evaluate the evolution of the carbon cycle through geologic times (Bocherens et al., 1993; Sinha and Stott, 1994; Stern at al., 1994; Ghosh et al., 1995; Beerling, 1997; Hasegawa et al., 1997; Beerling and Jolley, 1998; Gröcke, 1999; Arinobu et al., 1999; Utescher et al., 2000; Arens and Jahren, 2000; Beerling et al., 2001; Jahren et al., 2001; Gröcke, 2002; Ando et al., 2002; Strauss and Peters-Kottig, 2003; Heimhofer et al., 2003; Hasegawa et al., 2003; Jia et al., 2003; Magioncalda et al., 2004; Robinson and Hesselbo, 2004; Harris et al., 2004; Heimhofer et al., 2004). The bulk organic matter in the Diablito-1 and Gonzalez-1 samples displays $\delta^{13}C$ values around -27‰ (Appendix 1), which are typical for C_3 plants (Farquhar et al., 1989). The good correspondence between the marine and the terrestrial isotope data (Figure 12) provides support to the notion that a tight linkage exists between the oceans, the atmosphere, and land plants, indicating that perturbations occurring between 50 and 65 Ma were global in extent. However, the implication of the parallelism that exists between the marine and terrestrial $\delta^{13}C$ values relies on the assumption that $\delta^{13}C_{bulk}$ values truly reflect $\delta^{13}C_{plant}$ values. Although $\delta^{13}C_{bulk}$ values tend to reflect those of plan-derived organic matter, other effects, including the extent of microbial alteration, could potentially alter $\delta^{13}C_{bulk}$ values.

Moreover, the sedimentological analysis of the studied deposits suggests that some sediments accumulated in shallow freshwater environments (i.e., oxbow lakes), where the contribution of aquatic plants to the sedimentary organic pool could be significant. The influence of microbial degradation and aquatic vegetation on $\delta^{13}C_{bulk}$ values needs to be evaluated to assess the reliability of these values.

Several studies have addressed the effect of diagenesis through different approaches (Arens et al., 2000; Gröcke, 2002; Bergen and Poole, 2002; Beerling and Royer, 2002; Strauss and Peters-Kottig, 2003), but these studies rely on comparisons between $\delta^{13}C_{bulk}$ and $\delta^{13}C$ values of plant cuticles (e.g., Arens and Jahren, 2000) or woody fragments (Gröcke, 2002) or on evaluations of the level of microbial degradation inferred from molecular components (biomarkers) (Bergen and Poole, 2002; Poole et al., 2004). For instance, Arens et al. (2000) assumed that the only significant source of variation in $\delta^{13}C_{plant}$ values comes from variations in $\delta^{13}C_{CO2}$ values, with no further consideration on the potential effects of diagenesis. In contrast, Bergen and Poole (2002) identified high levels of organic matter alteration in fossilized woody fragments, which could potentially alter pristine $\delta^{13}C_{plant}$ values, thus constraining the use of $\delta^{13}C_{bulk}$ as a reliable proxy in estimating the evolution of the carbon cycle. To evaluate the role diagenesis and the sources of organic matter on $\delta^{13}C_{bulk}$ values, several biomarker ratios were employed in this study because of their demonstrated response to diagenesis and/or their specificity to different sources of organic matter (e.g., vascular plants, algae, bacteria).

These ratios were calculated from the relative abundances of the different compounds identified in the saturated fraction. The saturated fraction shows that n-alkanes display an overall odd-over-even predominance (Figure 15), which is usually associated with significant input of organic matter from terrestrial vascular plants (Gülz, 1994; Lichtfouse et al., 1994; Bechtel et al., 2003; Otto et al., 2005). Odd number long-chain n-alkanes are major components of plant cuticular waxes formed as a result of elongation and further decarboxylation from a fatty acid precursor (e.g., palmitate) (Harwood and Russell, 1984). Although this odd-over-even predominance of n-alkanes is a good indicator of terrestrial contributions, Peters et al. (2005) suggested that a better evaluation of the potential contribution of land plants to the bulk organic matter can be achieved with the carbon preference index (CPI) ratio, which is determined through the following equation:

$$CPI = \tfrac{1}{2} * (25+27+29+31+33)/(24+26+28+30+32) + \tfrac{1}{2} * (25+27+29+31+33)/(26+28+30+32+34) \quad (8)$$

The numbers in equation 8 represent the number of carbons in an n-alkane molecule. CPI values for the Gonzalez-1 and the Diablito-1 samples range from 1.24 to 1.92 and from 1.6 to 2.47, respectively (Appendix 1, Figures 20 and 21). While CPI values of the Gonzalez-1 samples increase with depth (Figure 21), those of the Diablito-1 samples show no trend and they fall within a narrow range (1.7-2.1), with the exception of the values at 470 m (Figure 20).

These CPI values obtained for the studied samples are lower than those commonly observed for extant vascular plants (van Dongen et al., 2006), which are commonly >3, but they do suggest significant contributions of organic matter derived from these higher plants. Typically, CPI values greater than 1 correspond to a predominantly land-plant input (Ficken et al., 2000; Schefuß et al., 2003; Muri et al., 2004; Stefanova, 2004; Peters et al., 2005; van Dongen, 2006; Eglinton et al., 2006). Although both n-alkane distribution and CPI values suggest the predominance of vascular plant-derived organic matter, the presence of short chain lipids in the saturated fraction in significant abundances (~80% in average, Figures 14 and 15) suggests other type of contributions different than those of terrestrial land plants. Short-chain lipids are commonly associated with the input of organic matter derived from freshwater photosynthetic algae and/or macrophytes (submerging/floating plants) (Cranwell et al., 1987; Mello and Maxwell, 1990; Bechtel et al., 2003; Muri et al., 2004; van Dogen et al., 2006). Because some oxic bacteria decompose organic matter when anoxic conditions are not rapidly reached, short-chain lipids could also come from such organisms (e.g., Cranwell et al., 1987; Bechtel et al., 2003), and their contributions to the studied sediments cannot be ruled out.

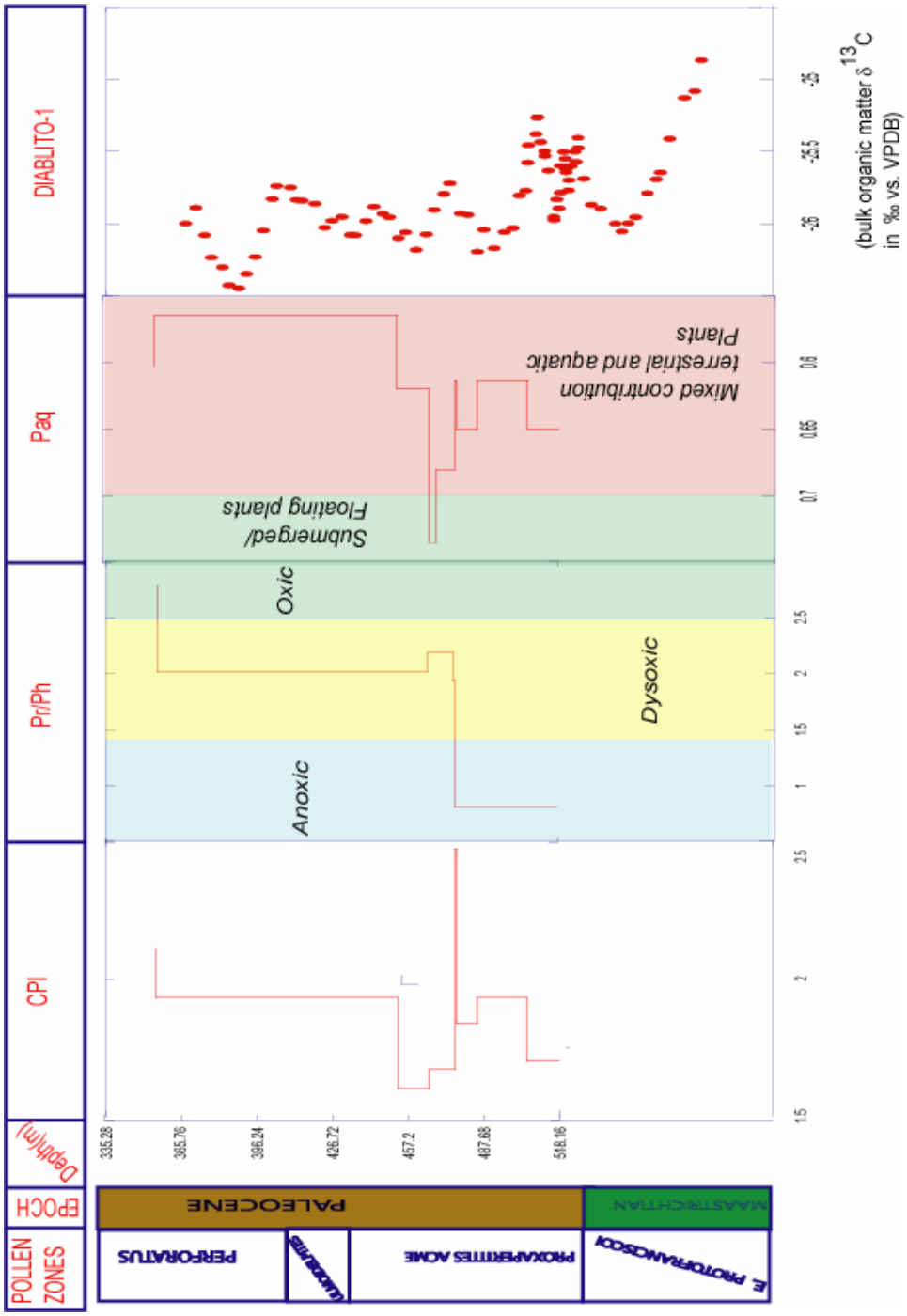

Figure 20. Stratigraphic variability of the Carbon Preference Index (CPI), pristane/phytane (Pr/Ph) ratio, aquatic/terrestrial plants (Paq) ratio, and carbon isotopic composition ($\delta^{13}C$) in the Diablito-1 well.

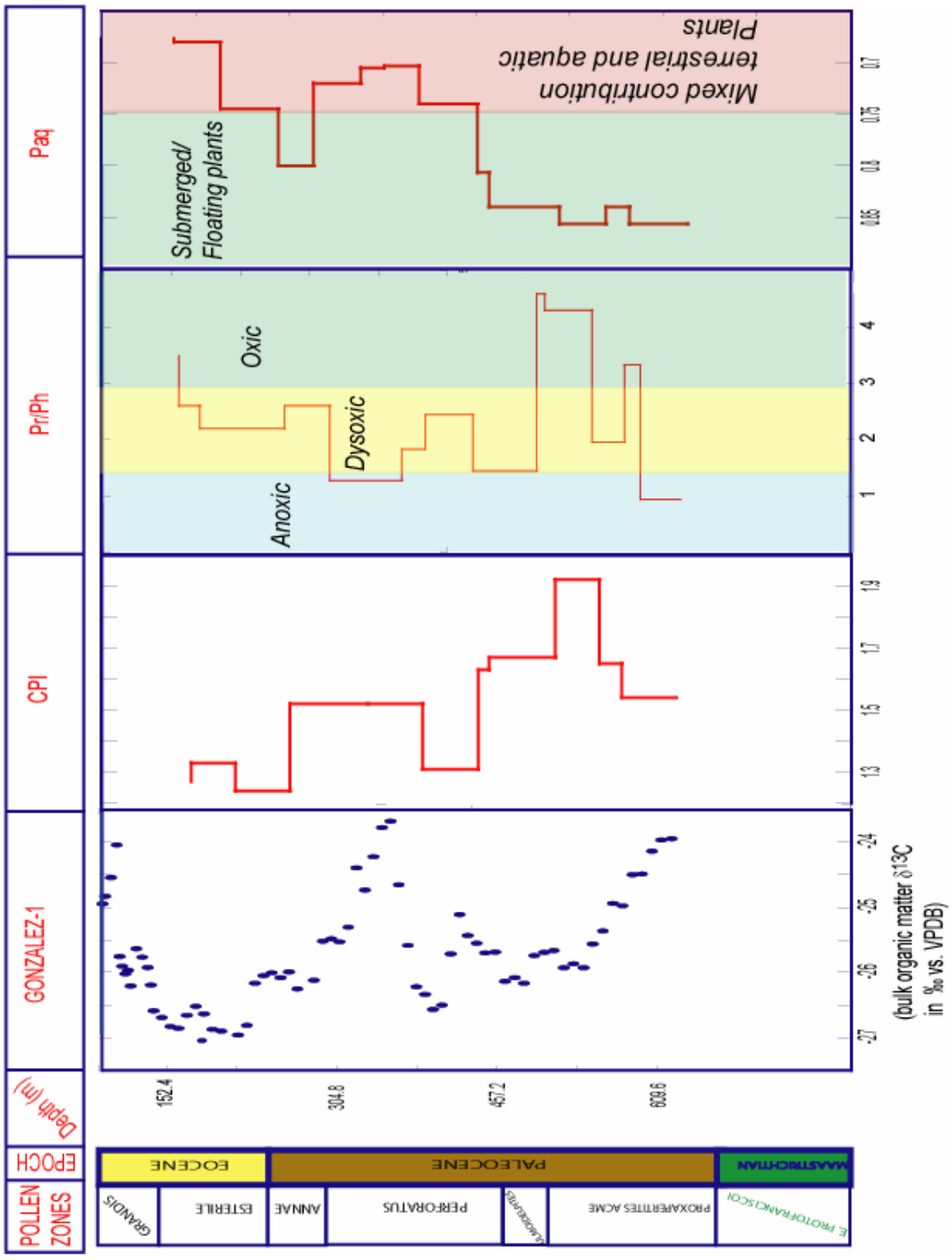

Figure 21. Stratigraphic variability of the Carbon Preference Index (CPI), pristane/phytane (Pr/Ph) ratio, aquatic/terrestrial plants (Paq) ratio, and carbon isotopic composition ($\delta^{13}C$) in the Gonzalez-1 well.

Despite the potential influence of lacustrine algae and/or bacterial organic matter, the odd-over-even predominance showed by the CPI index shows that, within the high molecular weight n-alkanes, land plant-derived organic matter contributed the most to the bulk of the straight-chain compounds. The compounds nC_{25}, nC_{27}, nC_{29}, and nC_{31} are the dominant compounds, rather than even number long-chain n-alkanes, which are synthesized by bacteria and marine organisms (Tissot and Welte, 1984; Peters et al., 2005; Killops and Killops, 2005). This predominance of terrestrial derived material is in agreement with the pollen data, which suggest a significant contribution from land plants.

Because of the abundance of short-chain lipids and their possible origin (freshwater photosynthetic organisms), the terrestrial/freshwater plants (P_{aq}) ratio developed by Ficken (2000) can be used to assess the source of most of the long-chain lipids preserved in the studied sediments. The P_{aq} ratio is defined as the ratio between the abundance of mid-chain n-alkanes (nC_{23}, nC_{25}) produced by submerging/floating freshwater plants (macrophytes) over the amount of long-chain n-alkanes ($nC_{27,}$ $nC_{29,}$ nC_{31}) produced by terrestrial plants:

$$\mathbf{P_{aq} = (23+25)/ (27+29+31)\ (9)}$$

P_{aq} values < 0.4 suggest a predominant terrestrial input, values > 0.75 reflect a primary submerging/floating plants contribution, and values between 0.4 and 0.75 reflect a mixture.

There is an overall trend to lower values with decreasing depth (age), indicating a transition towards more terrestrial conditions in younger samples (Appendix 1, and Figures 20 and 21). Diablito-1 samples (Appendix 2) display lower values relative to those determined for Gonzalez 1 samples (Appendix 2), suggesting a higher input of terrestrial plants to the bulk organic matter into the Cesar-Rancheria basin or the result of a poor preservation conditions (i.e., oxic conditions and/or bacterial reworking) in the Catatumbo basin (Gonzalez-1). This index, thus, suggests a mixed contribution of terrestrial and freshwater plants.

Supporting the conclusion that plant-derived organic matter is present in the studied sediments, sesquiterpenoids were identified in the saturated fraction (Figure 14 and Appendix 2). Bicyclic sesquiterpenoids have been identified in a variety of geological materials, from recent and ancient sediments to coals, oils, peats, ambers, and fossil resins (Otto et al., 1997; Otto and Simoneit, 2001; Bechtel et al., 2002 and 2003; Tuo and Philp, 2005; Hautevelle et al., 2006). Sesquiterpenoids are widely distributed among vascular plants, including both angiosperms and gymnosperms (Otto and Simoneit, 2001). The exception is cadalene, which is a group of compounds that appears to be related to gymnosperm-derived material (Otto et al., 1997; Bechtel et al., 2003). Although cadalene has been recognized as one of major components of resins in several conifer (gymnosperm) species (Phillip, 1985; Otto et al., 1997), it has also been reported to result from the degradation of resins produced by some angiosperm species (Otto et al., 1997).

Both cadalene and the C_{16} sesquiterpane (Tp_1 and Tp_2, Figure 14) were identified in the studied samples, possibly suggesting the contribution of gymnosperm-derived organic matter to the studied sediments. In addition to the possible contribution of gymnosperms, the triterpenoids found in the saturated fraction correspond to lupane- (L_2) and normoretane-type (L_1) compounds (Figure 14 and Appendix 2), which are associated with angiosperms (Sukh Dev, 1989; Bechtel et al., 2003; Peters et al., 2005). These two compounds have been found in leaf, wood, root, and bark tissues of these plants (Sukh Dev, 1989; Bechtel et al., 2003). The presence of these compounds in the studied sediments, coupled with the presence of sesquiterpenoids, supports the CPI data, suggesting that vascular plants were an importance source of the organic matter in the Gonzalez-1 and Diablito-1 sediments.

4.2. PRESERVATION OF THE ORGANIC MATTER

Although CPI values reflect a slightly dominant contribution from terrestrial plants to the bulk organic matter, the predominance of short-chain over long-chain n-alkanes could also result from a poor preservation of the heavier compounds. Redox conditions govern to a large extent the preservation potential of organic matter, with oxic conditions leading to poor preservation. Because of his sensitivity to redox conditions, the Pr/Ph ratio can be used to evaluate the effect of oxicity during the accumulation of the studied samples (Didyk et al., 1978: Bechtel et al., 2003).

Variations in the Pr/Ph ratios for the studied samples (Figures 20 and 21) suggest the existence of two different redox regimes governing the depositional settings of the two basins (Catatumbo and Cesar-rancheria basins for Gonzalez-1 and Diablito-1, respectively). Diablito-1 samples, covering the time interval from ~66 to 57 M.a., show Pr/Ph vales indicative of a change from anoxic (below 450 m) to dysoxic (450-350 m) and possibly oxic conditions (above 350 m). Gonzalez-1 Pr/Ph values suggest that the organic matter in those sediments was deposited under dysoxic to oxic conditions between 450 and 600 m (Catatumbo Formation), changing to anoxic/dysoxic conditions between 450 and 300 m (Barco Formation), and shifting towards more oxic conditions at depths above 300 m of the section (Cuervos Formation). Such displacement of the column of oxic water downward could account for the inverse relationship that exists between asphaltene contents and Pr/Ph values (Figure 22). Oxic conditions reduce the preservation potential of most organic compounds, even those typically resistant to degradation due to intense microbial activity (Didyk et al., 1978; Peters et al., 2005). Asphaltenes are considered some of the most resistant compounds to microbial alteration within the SOM (Tissot and Welte, 1984; Killops and Killops, 2005) because of their inert-like behavior. Consequently, a relative increase in their abundance would occur under oxic conditions as a result of the degradation of other less resistant compounds, thus explaining the inverse correlation found in the data.

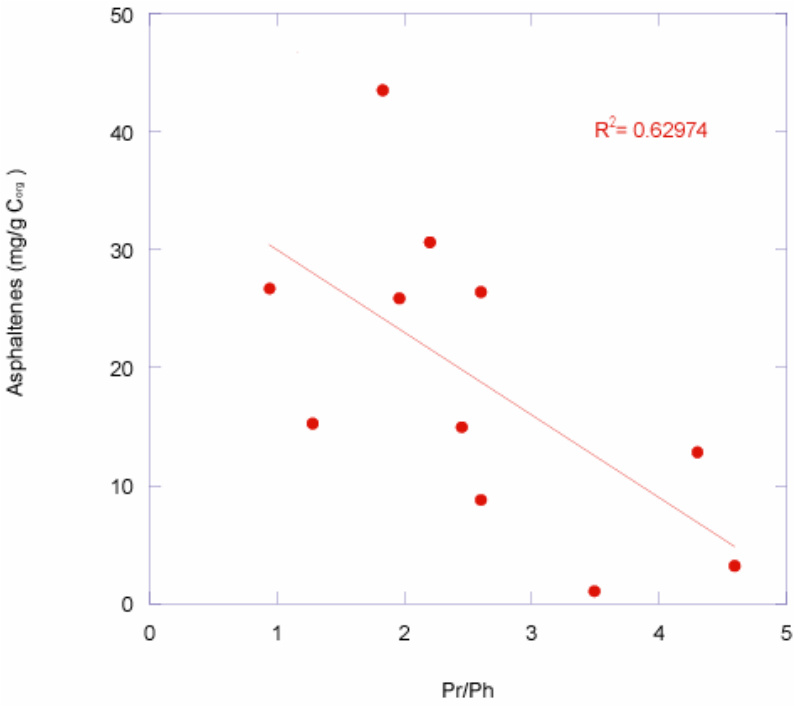

Figure 22. Cross correlation of asphaltenes content vs. Pr/Ph values. The relationship is significant (r^2= 0.62, p< 0.0001).

This relative increase of asphaltenes under oxic conditions suggests the degradation of less resistant compounds by microorganisms, which can be evaluated though the compounds that they produce (Peters et al., 2005). Hopanes (H1-H8, Appendix 2 and Figure 14) are important constituents of the saturated fraction in the studied samples, and these compounds are associated with microbial contributions to the bulk organic matter (Peters et al., 2005). For that reason, hopanes abundances can be used to estimate the intensity of biomass degradation by using the ratio ββ/ (ββ+ αβ) hopanes (Figure 23) (Mackenzie et al., 1981; Bechtel et al., 2003; van Dongen et al., 2006).

Commonly, low ββ/ (ββ+ αβ) values (below 0.5) are indicators of moderate to high degration of organic matter, because αβ hopanes are more kinetically stable as diagenesis degrades sedimentary organic matter. Figure 23 shows that Gonzalez-1 and Diablito-1 samples display parallel trends, which suggests that, despite of the differences in preservation and contribution from terrestrial sources, the organic matter at both sites experienced similar degradation patterns.

4.3. EVALUATION OF $\delta^{13}C_{bulk}$ VALUES

The CPI values and the sesquiterpenoid and lupanoid abundances confirm the assumption of a predominant terrestrial origin for the bulk organic matter in the studied sediments, which is also supported by the pollen data. However, the predominant dysoxic-oxic conditions during deposition (as determined from the Pr/Ph values) and the significant levels of biomass degradation during diagenesis (as interpreted from ββ/ (ββ+ αβ) values) could imply that the measured $\delta^{13}C_{bulk}$ is different than the original $\delta^{13}C_{plant}$ values. To evaluate this potential effect, $\delta^{13}C_{bulk}$ values were plotted against our diagenetic proxies (i.e., Pr/Ph, C_{org}, and ββ/ (ββ+ αβ). In addition, $\delta^{13}C_{bulk}$ values were also plotted against CPI and P_{aq} to evaluate the possible influence of the type of organic matter on the observed trend in $\delta^{13}C_{bulk}$ values.

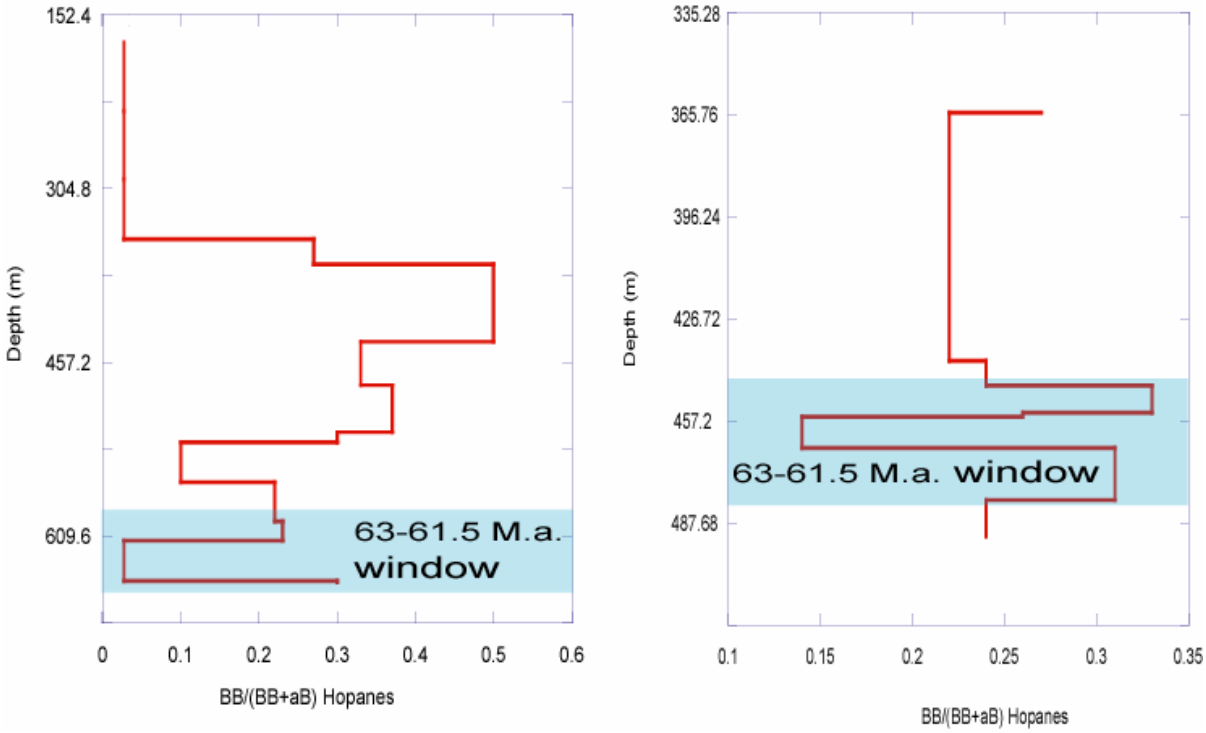

Figure 23. Distribution of ββ/ (ββ+ αβ) hopanes ratios in the Gonzalez-1 (left graph) and Diablito-1 (right graph) sections.

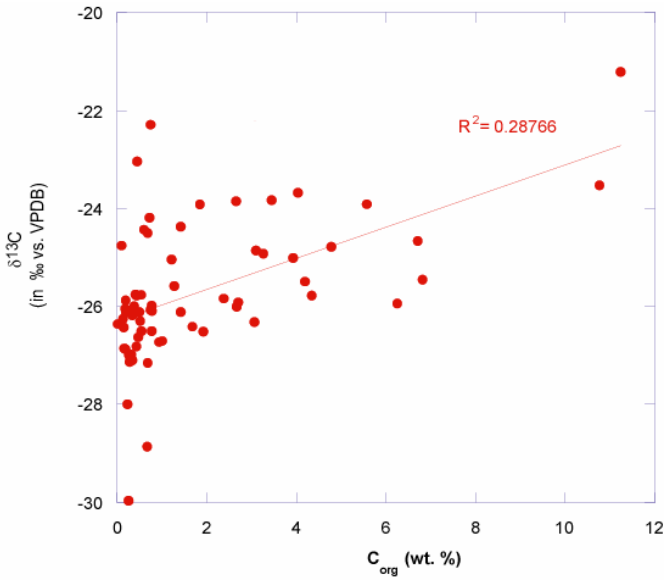

Figure 24. Cross correlation of $\delta^{13}C_{bulk}$ values vs. composite C_{org} abundances in the Gonzalez-1 and Diablito-1 samples. The relationship is significant ($p<0.0001$).

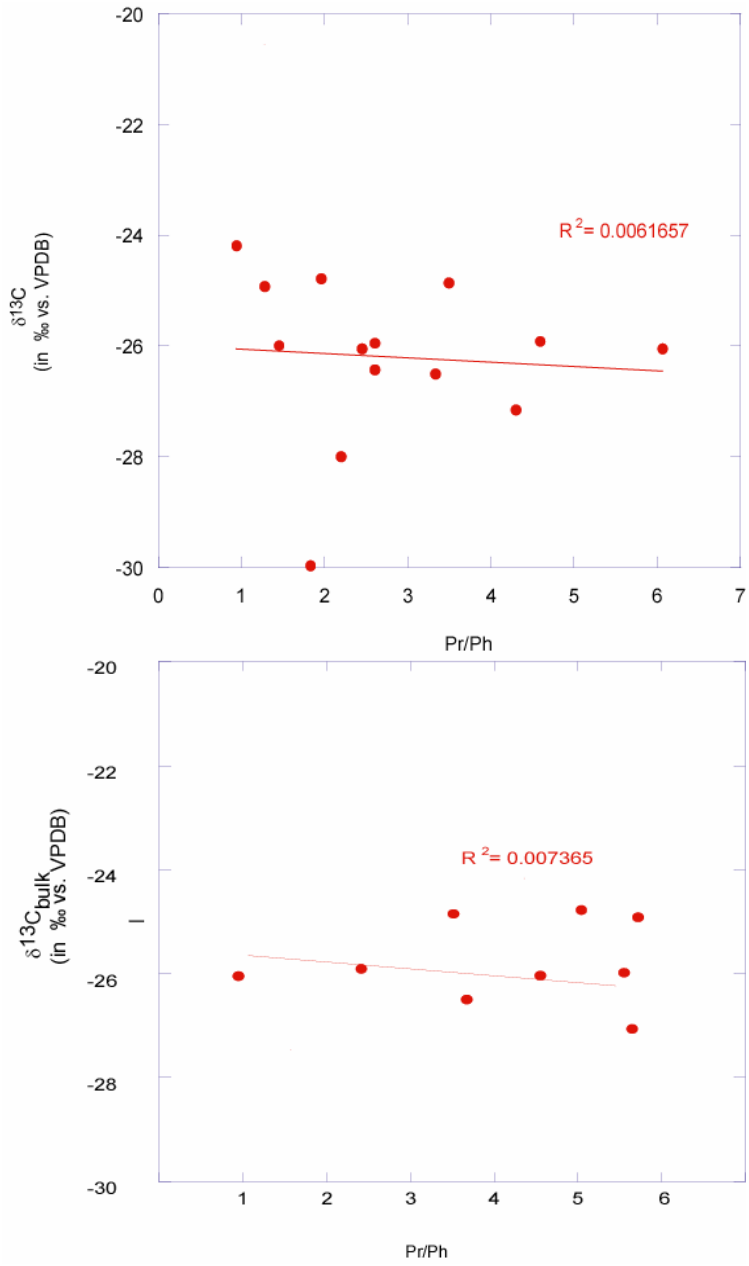

Figure 25. Cross correlation of $\delta^{13}C_{bulk}$ vs. Pr/Ph values for the Gonzalez-1 (upper panel) and Diablito-1 (lower panel) samples. The relationship is not significant ($p<0.87$ and 0.96, respectively).

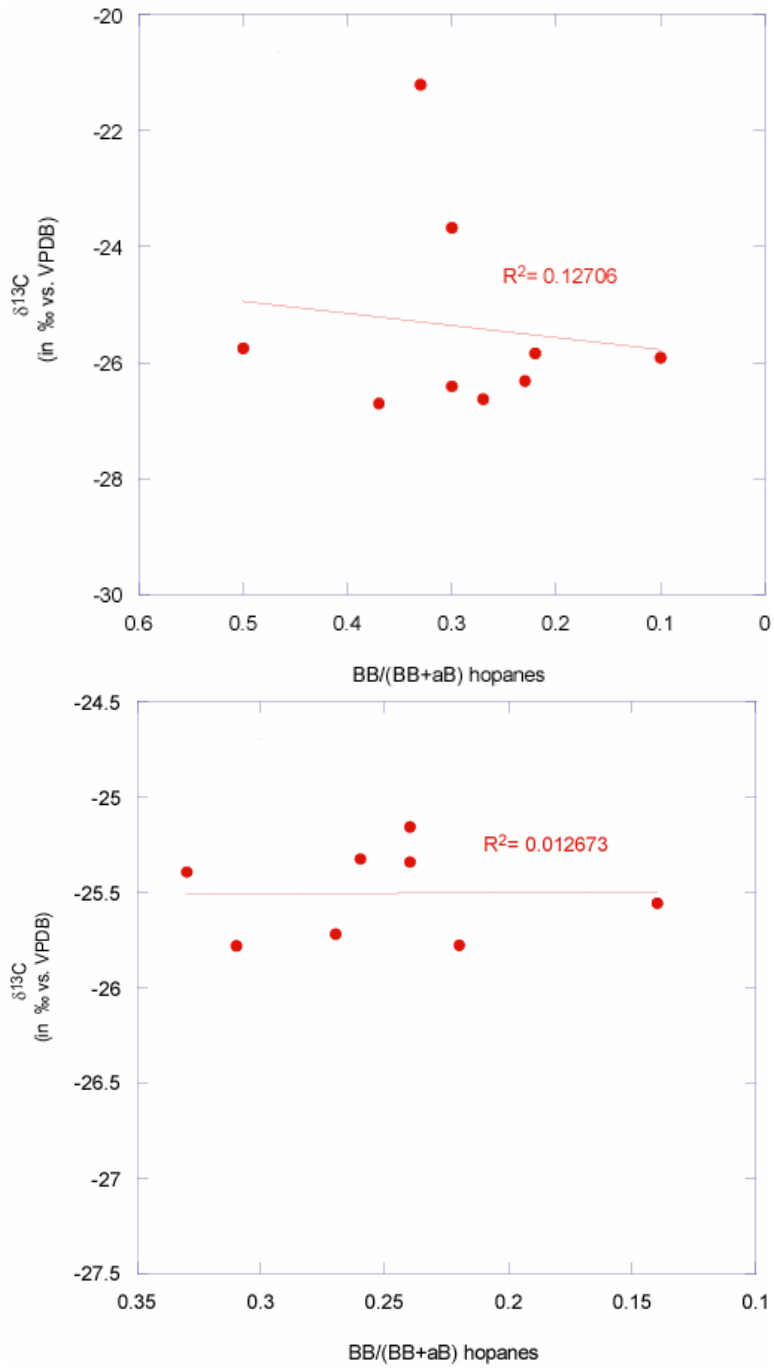

Figure 26. Cross correlation of $\delta^{13}C_{bulk}$ vs. ββ/ (ββ+ αβ) values for the Gonzalez-1 (upper graph) and Diablito-1 (lower graph) samples. The relationships are not significant ($p<0.7446$ and 0.9762, respectively).

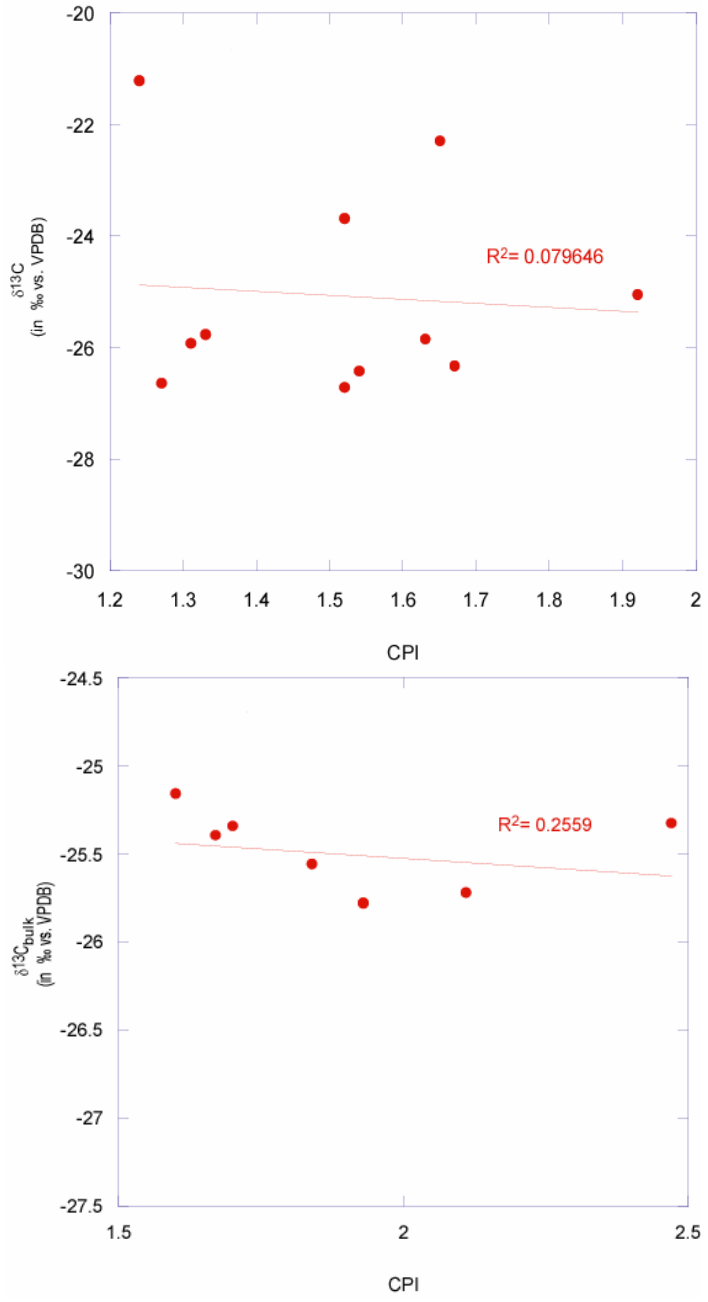

Figure 27. Cross correlation of $\delta^{13}C_{bulk}$ vs. CPI values for the Gonzalez-1 (upper panel) and Diablito-1 (lower panel) samples. The relationships are not significant ($p<0.81$ and 0.54, respectively).

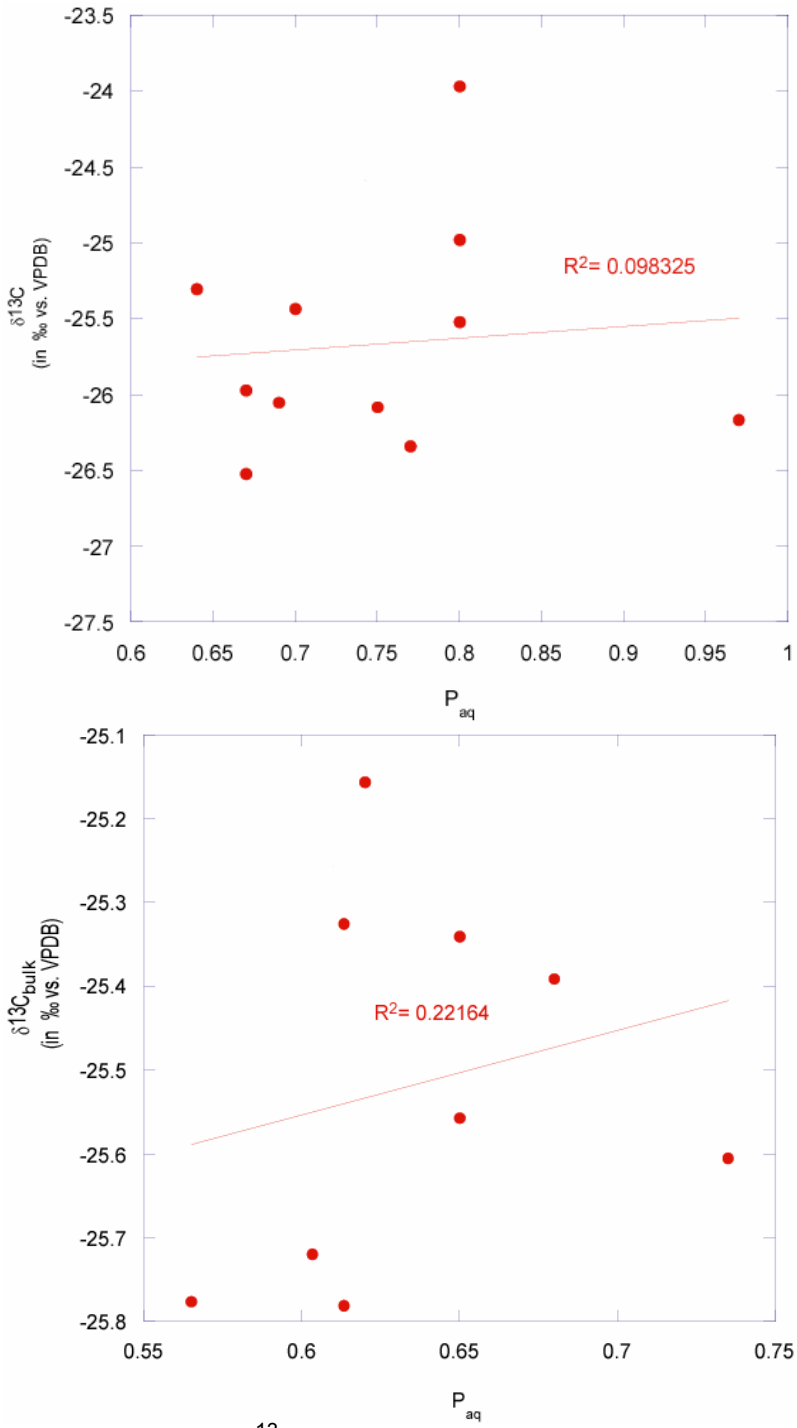

Figure 28. Cross correlation of $\delta^{13}C_{bulk}$ vs. P_{aq} values for the Gonzalez-1 (upper panel) and Diablito-1 (lower panel) samples. The relationships are not significant ($p<0.77$ and 0.076, respectively).

No significant correlation exists between each of the parameters analyzed and $\delta^{13}C_{bulk}$ values (Figures 24-28), suggesting that neither depositional environment nor the degree of biomass alteration during diagenesis have significantly altered the measured $\delta^{13}C_{bulk}$ values. These results do not agree with other results (e.g., Gröcke, 2002; Bergen and Poole, 2002), suggesting that $\delta^{13}C_{bulk}$ values are strongly affected by C_{org} content and diagenesis. In contrast, results from this study indicate that $\delta^{13}C_{bulk}$ values could be used for chronostratigraphic purposes, since they are possibly close to those of the ancient plants. However, when combining Diablito-1 and Gonzalez-1 data to generate a composite $\delta^{13}C_{bulk}$ curve, some noise in the signal emerges, which is associated with the Diablito-1 isotope values (Figure 29). This noise is likely unrelated to diagenesis, since the Diablito-1 data has higher CPI (higher land plant contribution) and similar ββ/(ββ+ αβ) values in comparison with Gonzalez-1 data. These higher CPI could imply that differences in the amount of land plant contribution to the preserved organic matter might be the cause for the noise in the Diablito-1 samples.

The absence of correlation between the $\delta^{13}C_{bulk}$ values and biomass alteration (Figure 26), the contribution of vascular and non-vascular plant-derived organic matter (Figure 27), and the oxygen levels during deposition (Figure 25) implies that the secular shifts in $\delta^{13}C_{bulk}$ values are probably related to changes in original $\delta^{13}C_{plant}$ values and not produced by diagenesis or varying contributions of different organic matter sources.

Therefore, the shifts in isotopic values that occurred in the Colombian tropics (Gonzalez-1 and Diablito-1 sections) between 65 and 50 M.a. reflect the shifts in isotopic values recorded in marine deposits (Zachos et al., 2001), thus confirming a connection between the oceans and terrestrial biomass via the atmosphere. This connectivity implies that long-term changes in marine $\delta^{13}C_{carbonate}$ values should cause similar changes in $\delta^{13}C_{plant}$ values, which are ultimately reflected in $\delta^{13}C_{bulk}$ values (e.g., Figure 30).

Figure 30 shows that there is a consistent difference between $\delta^{13}C_{bulk}$ and $\delta^{13}C_{carbonate}$ values. This difference of about –27‰ is also observed in modern settings (Farquhar et al., 1989; Strauss and Peters-Kottig, 2003). However, Beerling and Royer (2002) and Strauss and Peters-Kottig (2003) suggest that this difference was probably not consistent in the geologic past as a result of different oxygen/carbon dioxide ratios in the atmosphere, which were more significant in the Paleozoic (360-240 M.a.). Although this study does not address this issue since oxygen/carbon dioxide ratios between 50 and 65 Ma were not significantly different relative to today's conditions, future research should focus on evaluating this potential effect

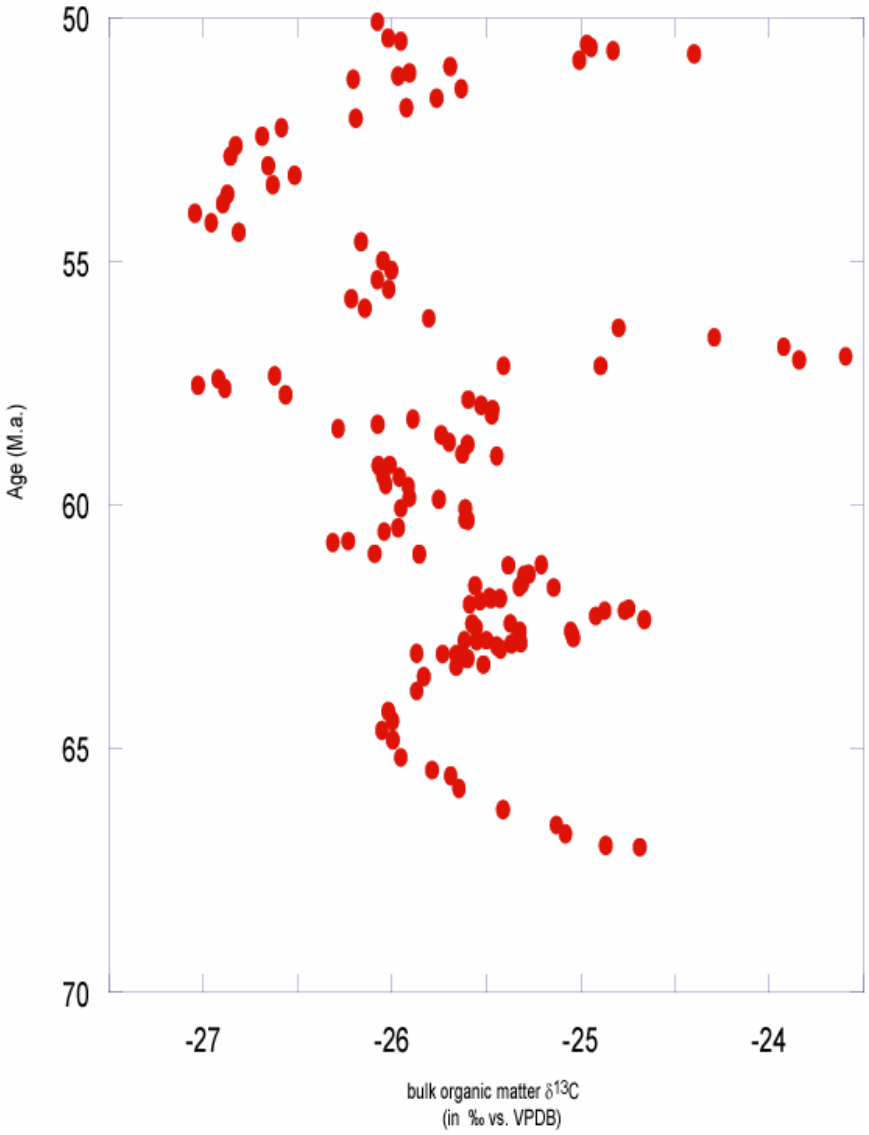

Figure 29. Gonzalez-1 and Diablito-1 composite $\delta^{13}C_{bulk}$ values for the 65-50 M.a. time interval. A five-point moving average filter was applied to the combined data.

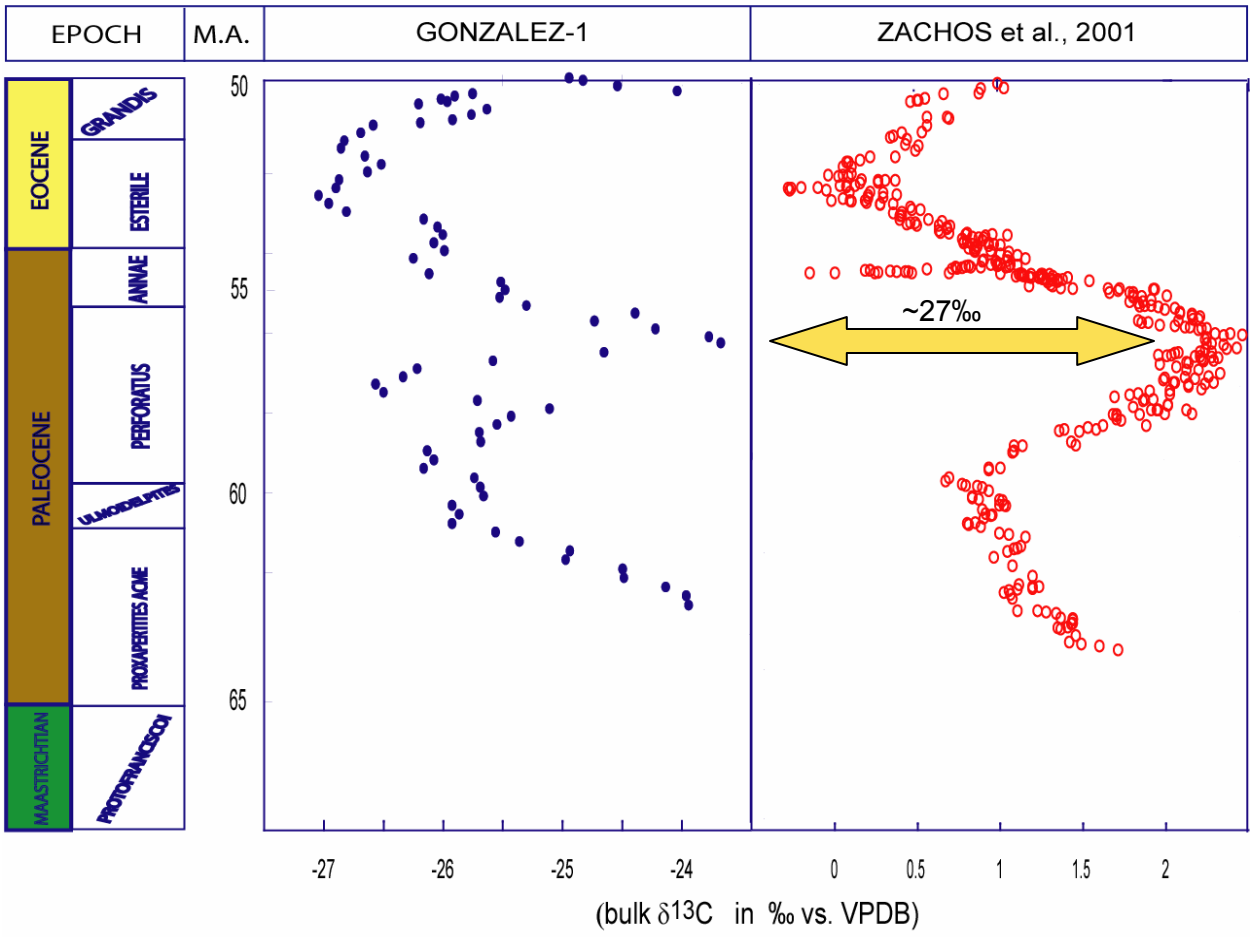

Figure 30. Comparison between the carbon isotopic composition of terrestrial organic matter (Gonzalez-1) and marine carbonates (Zachos et al., 2001) during the Paleocene-early Eocene. Notice that the difference in isotopic composition (yellow double-head arrow) is similar to the modern average difference between modern carbonates and extant terrestrial biomass.

5. CONCLUSIONS

The secular variations in the carbon cycle that occurred between 65 and 50 M.a., as inferred from marine $\delta^{13}C_{carbonate}$ values (Zachos et al., 2001), were also recognized in the $\delta^{13}C_{bulk}$ values of terrestrial sequences accumulated in the South American tropics during the same time interval. The different biomarker ratios utilized in the present study (CPI, Pr/Ph, Paq, and ββ/ (ββ+ αβ) hopanes) show no significant correlation with $\delta^{13}C_{bulk}$ values, thus suggesting that the secular changes in $\delta^{13}C_{bulk}$ values were not caused by changes in depositional environment, oxygen levels, type of land plant inputs, or degree of biomass alteration. The similarity in isotopic trends reinforces the assumption of an isotopic connection between the oceans and the terrestrial biomass via the atmosphere, thus making $\delta^{13}C_{bulk}$ values a potentially reliable tool for stratigraphic correlations between marine and terrestrial sequences.

6. REFERENCES

Ando, A., Kakegawa, T., Takashima R., Saito, T., (2002) New perspective on Aptian carbon isotope stratigraphy: data from $\delta^{13}C$ records of terrestrial organic matter. *Geology*, 30(3), p. 227-230.

Arens, N., Jahren, H., Amundson, R., (2000) Can C_3 Plants faithfully record the carbon isotopic composition of atmospheric carbon dioxide? *Paleobiology*, 26(1), p. 137-164.

Arens, N., Jahren, H., (2000) Carbon isotope excursion in the atmospheric CO_2 at the Cretaceous-Tertiary boundary: evidence from terrestrial sediments. *Palaios*, 15, p. 314-322.

Arinobu, T., Ishiwatari, R., Kahio, K., Lamolda, M., (1999) Spike of pyrosynthetic polycyclic aromatic hydrocarbons associated with and abrupt decrease in $\delta^{13}C$ of a terrestrial biomarker at the Cretaceous-Tertiary boundary at Caravaca, Spain. *Geology*, 27(8), p. 723-726.

Bechtel, A., Sachsenhofer, R., Gratzer, R., Lucke, A., Puttmann, W., (2002) Parameters determining the carbon isotopic composition of coal and fossil wood in the Early Miocene Oberdorf lignite seam (Styrian basin, Austria). *Organic Geochemistry*, 33, p. 1001-1024.

Bechtel, A., Sachsenhofer, R., Markic, M., Gratzer, R., Lucke, A., Puttmann, W., (2003) Paleoenvironmental implications from biomarker and stable isotope investigations on the Pliocene Velenje lignite seam (Slovenia). *Organic Geochemistry*, 34, p. 1277-1298.

Beerling, D., (1997) Interpreting environmental and biological signals from the stable carbon isotope composition of fossilized organic and inorganic carbon. *Journal of the Geological Society, London.*, 154, p. 303-309.

Beerling, D., Jolley, D., (1998) Fossil plants record an atmospheric $^{12}CO_2$ and temperature spike across the Paleocene-Eocene transition in NW Europe. *Journal of the Geological Society, London.*, 155, p. 591-594.

Beerling, D., Lomax, B., Upchurch Jr., B., Nichols, D., Pillmore, C., Handley, L., Scrimgeour, C. , (2001) Evidence for the recovery of terrestrial ecosystems ahead of marine primary production following the biotic crisis at the Cretaceous-Tertiary boundary. *Journal of the Geological Society, London.*, 158, p. 737-740.

Beerling, D., Royer, D., (2002) Fossil plants as indicators of the Phanerozoic global carbon cycle. *Annual Review of Earth and Planetary Sciences*, 30, p. 527-556.

Beerling, D., Lomas, M., Gröcke, D., (2002) On the nature of methane gas-hydrate dissociation during the Toarcian and Aptian Oceanic Anoxic Events. *American Journal of Science*, 302, p. 28-49.

Bergen, F., Poole, I., (2002) Stable carbon isotopes of wood: a clue to paleoclimate? *Palaeogeography, Palaeoclimatology, Palaeoecology*, 182, p. 31-45.

Berner, R., (2006) Carbon, sulfur and O_2 across the Permian-Triassic boundary. *Journal of Geochemical Exploration*, 88, p. 416-418.

Bocherens, H., Friis, E., Mariotti, A., Pedersen, K. R., (1993) Carbon isotopic abundances in Mesozoic and Cenozoic fossil plants: palaeoecological implications. *Lethaia*, 26, p. 347-358.

Böhm, F., Joachismki, M., Lehnert, H., Morgenroth, G., Kretschemer, W., Vacelet, J., Dullo, W., (1996) Carbon isotope records from extant Caribbean and South Pacific sponges: evolution of $\delta^{13}C$ in surface water DIC. *Earth and Planetary Science Letters*, 139, p. 291-303.

Corfield, R., Norris, R., (1998) The oxygen and carbon isotopic context of the Paleocene/Eocene epoch boundary. *In: Aubry, M., Lucas, S., Berggren, W. (ed.). Late Paleocene-Early Eocene climatic and biotic events in the marine and terrestrial records. Columbia University Press, New York.*, p. 124-136.

Craig, H., (1953) The geochemistry of stable carbon isotopes. *Geochemica et Cosmochemica Acta*, 3, p. 53-92.

Cranwell, P., Eglington, G., Robinson, N., (1987) Lipids of aquatic organisms as potential contributors to lacustrine sediments-II. *Organic Geochemistry*, 11(6), p.513-527.

Didyk, B., Simoneit, B., Brassell, S., Eglinton, G., (1978) Organic geochemical indicators of palaeoenvironmental conditions of sedimentation. *Nature*, 272, p. 216-222.

Eglinton, L., Lim, D., Slater, G., Osinski, G., Whelan, J., Douglas, M., (2006) Organic geochemical characterization of a Miocene core sample from Haughton impact structure, Devon Island, Nunavut, Canadian High Artic. *Organic Geochemistry*, 37, p. 688-710.

Farquhar, G., Ehleringer, J., Hubick, K., (1989) Carbon isotope discrimination and photosynthesis. *Annual Review of Plant Physiology and Plant Molecular Biology.*, 40, p. 503-537.

Ficken, K., Li, B., Swain, D., Eglinton, G., (2000) An n-alkane proxy for the sedimentary input of submerged / floating freshwater aquatic macrophytes. *Organic Geochemistry*, 31, p. 745-749.

Freeman, K., Colarusso, L., (2001) Molecular and isotopic records of C_4 grassland expansion in the Late Miocene. *Geochemica et Cosmochemica Acta*, 65(9), p. 1439-1454.

Galimov, E., (1985) On fractionation of isotopes by biological organisms *In: The biological fractionation of isotopes.*, Academic Press Inc. pp. 261.

Ghosh, P., Bhattacharya, S., Jani, R., (1995) Palaeoclimate and palaeovegetation in central India during the Upper Cretaceous based on stable isotope composition of the paleosol carbonates. *Palaeogeography, Palaeoclimatology, Palaeoecology*, 114, p. 285-296.

Glumac, B., Walker, K., (1998) A Late Cambrian positive carbon-isotope excursion in the southern Appalachians: relation to biostratigraphy, sequence stratigraphy, environments of deposition, and diagenesis. *Journal of Sedimentary Research*, 68(6), p. 1212-1222.

Gröcke, D., (1998) Carbon-isotope analyses of fossil plants as a chemostratigraphic and paleoenvironmental tool. *Lethaia*, 31, p. 1-13.

Gröcke, D., Hesselbo, S., Jenkyns, H., (1999) Carbon-isotope composition of Lower Cretaceous fossil wood: ocean-atmosphere chemistry and relation to sea-level change. *Geology*, 27(2), p.155-158.

Gröcke, D., (2002) The carbon isotope composition of ancient CO_2 based on higher plant organic matter. *Philosophycal Transactions of the Royal Society, London. A* 360, p. 633-658.

Gülz, P., (1994) Epicuticular leaf waxes in the evolution of the plant kingdom. *Journal of Plant Physiology*, 143, p. 453-464.

Harrington, G., Jaramillo, C. A., (2007) Paratropical floral extinction in the Late Paleocene-Early Eocene. *Journal of the Geological Society, London.*, 164, p. 323-332.

Harris, N., Freeman, K., Pancost, R., White, T., Mitchell, G., (2004) The character and origin of lacustrine source rocks in the Lower Cretaceous synrift section, Congo Basin, west Africa. *American Association of Petroleum Geologist Bulletin*, 88(8), p. 1163-1184.

Hartgers, W.A., Sinninghe, J.S., Requejo, A. J., Allan, J., Hayes, J.M., de Leeuw, J.W., (1994) Evidence for only minor contribution from bacteria to sedimentary organic carbon. *Nature*, 369, p. 224-227.

Harwood, J., Russel, N., (1984) *Lipids in plants and microbes. George Allen & Unwin Limited, London*, pp. 162.

Hasegawa, T., (1997) Cenomanian-Turonian carbon isotope events recorded in terrestrial organic matter from northern Japan. *Palaeogeography, Palaeoclimatology, Palaeoecology*, 130, p. 251-273.

Hasegawa, T., Pratt, L., Maeda, H., Shigeta, Y, Okamoto, T., Kase, T., Uemura, K., (2003) Upper Cretaceous stable carbon isotope stratigraphy of terrestrial organic matter from Sakhalin, Russian far east: a proxy for the isotopic composition of paleoatmospheric pCO_2. *Palaeogeography, Palaeoclimatology, Palaeoecology*, 189, 97-115.

Hautevelle, Y., Michels, R., Malartre, F., Trouiller, A., (2006) Vascular plants biomarkers as proxies for palaeoflora and palaeoclimatic changes at the Dogger / Malm transition of the Paris Basin (France). *Organic Geochemistry*, 37, p. 610-625. .

Hayes, J., Strauss, H., Kaufman, A., (1999) The abundance of ^{13}C in marine organic matter and isotopic fractionation in the global biogeochemical cycle of carbon during the past 800 Ma. *Chemical Geology*, 161, p. 103-125.

Hayes, J., (2001) Fractionation of carbon and hydrogen isotopes in biosynthetic processes. *In: Valley, J., Cole, D. (ed). Stable isotope geochemistry. Reviews in Mineralogy and Geochemistry*, 43, p. 225-277.

Heimhofer, U., Hochuli, P., Burla, S., Andersen, N., Weissert, H., (2003) Terrestrial carbon-isotope records from coastal deposits (Algarve, Portugal): a tool for chemostratigraphic correlation on an intrabasinal and global scale. *Terra Nova*, 15(1), p. 8-13.

Heimhofer, U., Hochuli, P., Herrle, J., Andersen, N., Weissert, H., (2004) Abscence of major vegetation and paleoatmospheric pCO_2 changes associated with oceanic anoxic event 1a (Early Aptian, SE France). *Earth and Planetary Science Letters*, 223, p. 303-318.

Hesselbo, S., Robinson, S., Surlyk, F., Piasecki, S., (2002) Terrestrial and marine extinction at the Triassic-jurassic boundary synchronized with major carbon cycle perturbation: a link to initiation of massive volcanism? *Geology*, 30(3), p. 251-254.

Hollis, C., Dickens, G., Field, B., Jones, C., Strong, P., (2005) The Paleocene-Eocene transition at Mead Stream, New Zealand: a southern Pacific record of Early Cenozoic global change. *Palaeogeography, Palaeoclimatology, Palaeoecology*, 215, p. 313-343.

Jahren, H., Arens, N. C., Sarmiento, G., Guerrero, J., Amundson, R., (2001) Terrestrial record of methane hydrate dissociation in the Early Cretaceous. *Geology*, 29(2), p. 159-162.

Jahren, H., Conrad, C., Arens, N. C., Mora, G., Lithgow-Bertelloni, C., (2005) A plate tectonic mechanism for methane hydrate release along subduction zones. *Earth and Planetary Science Letters*, 236, p. 691-704.

Jenkyns, H., (2003) Evidence for rapid climate change in the Mesozoic-Paleogene greenhouse world. *Philosophycal Transactions of the Royal Society, London*, 361, p. 1885-1916.

Jia, G., Peng, P., Zhao, Q., Jian, Z., (2003) Changes in terrestrial ecosystems sice 30 M.a. in east Asia: stable isotope evidence from black carbon in the south China Sea. *Geology*, 31(12), p. 1093-1096.

Kaiser, S., Steuber, T., Becker, R. T., Joachismki, M., (2006) Geochemical evidence for major environmental change at the Devonian-Carboniferous boundary in the Carnic Alps and the Rhenish Massif. *Palaeogeography, Palaeoclimatology, Palaeoecology*, 240, p. 146-160.

Killops, S., Killops, V., (2005) *Introduction to Organic Geochemistry. Blackwell publishing, London*, pp. 393.

Koch, P., Zachos, J., Gingerich, P., (1992) Correlation between isotope records in marine and continental carbon reservoirs near the Paleocene/Eocene boundary. *Nature*, 358, p. 319-322.

Koch, P., (1998) Isotopic reconstruction of past continental environments. *Annual Review of Earth and Planetary Sciences*, 26, p. 573-613.

Kump, L., Arthur, M., (1999) Interpreting carbon-isotope excursions: carbonates and organic matter. *Chemical Geology*, 161, p. 181-198.

Lichtfouse, É., Elbisser, B., Balesdent, J., Mariotti, A., Bardoux, G. , (1994) Isotope and molecular evidence for direct input of maize leaf wax n-alkanes into crop soils. *Organic Geochemistry*, 22(2), p. 349-351.

MacKenzie, A., Patience, R., Maxwell, J. R., (1981) Molecular changes in the maturation of sedimentary organic matter. *In: Atkinson, G., Zuckerman, J. (Eds.), Origin and Chemistry of Petroleum. Pergamon Press, Oxford*, p. 1-31.

Magioncalda, R., Dupuis, C., Smith, T., Steurbaut, E., Gingerich, P. , (2004) Paleocene-Eocene carbon isotope excursion in organic carbon and pedogenic carbonate: direct comparisson in a continental stratigraphic section. *Geology*, 32(7), p. 553-556.

Mello, M., Maxwell, J., (1990) Organic geochemical and biological marker characterization of source rocks and oils derived from lacustrine environments in the brazilian continental margin. *In: Lacustrine Basin Exploration (Katz, B. ed.). American Association of Petroleum Geologist memoir, 50*, p. 77-97.

Muri, G., Wakeham, S., Pease, T., Faganeli, J., (2004) Evaluation of lipid biomarkers as indicators of changes in organic matter delivery to sediments from Lake Planina, a remote mountain lake in NW Slovenia. *Organic Geochemistry*, 35, p. 1083-1093.

Norris, R., Kroon, D., Huber, B., Erbacher, J., (2001) Cretaceous-Paleogene ocean and climate change in the subtropical North Atlantic. *Geological Society, London, Special Publications*, 183, p. 1-22.

Otto, A., Walther, H., Püttmann, W., (1997) Sesqui-and diterpenoid biomarkers preserved in taxodium-rich Oligocene oxbox lake clays, Weisselster Basin, Germany. *Organic Geochemistry*, 26(1/2), p. 105-115.

Otto, A., Simoneit, B., (2001) Chemosystematics and diagenesis of terpenoids in fossil conifer species and sediment from the Eocene Zeitz Formation, Saxony, Germany. *Geochemica et Cosmochemica Acta*, 65(20), p. 3505-3527.

Otto, A., Simoneit, B., Rember, W., (2005) Conifer and angiosperm biomarkers in clay sediments and fossil plants from the Miocene Clarkia Formation, Idaho, USA. *Organic Geochemistry*, 36, p. 906-922.

Pearson, P., Palmer, M. , (2000) Estimating Paleogene atmospheric pCO_2 using boron isotope analysis of foraminifera. Transactions of the Geological Society in Stockholm, 122(1), p. 127-128.

Peters, K., Walters, C., Moldowan, M., (2005) *The Biomarker guide. Cambridge university press, New York,* pp. 1155.

Philp, R.P., (1985) *Fossil fuel biomarkers. Applications and spectra*. Methods in Geochemistry and Geophysics*, 23.* Elsevier, Amsterdam*,* p.244

Poole, I., van Bergen, P., Kool, J., Schouten, S., Cantrill, D., (2004) Molecular isotopic heterogeniety of fossil organic matter: implications for $\delta^{13}C_{biomass}$ and $\delta^{13}C_{palaeoatmosphere}$ proxies. *Organic Geochemistry*, 35, p. 1261-1274.

Robinson, S., Andrews, J., Hesselbo, S., Radley, J., Dennis, P., Harding, I., Allen, P., (2002) Atmospheric pCO_2 and depositional environment from stable-isotope geochemistry of calcrete nodules (Barremian, Lower Cretaceous, Wealden Beds, England). *Journal of the Geological Society, London.*, 159, p. 215-224.

Robinson, S., Hesselbo, S., (2004) Fossil-wood carbon-isotope stratigraphy of the non-marine Wealden Group (Lower Cretaceous, southern England). *Journal of the Geological Society, London.*, 161, p. 133-145.

Rost, B., Riebesell, U., Burkhardt, S., (2003) Carbon acquisition of bloom-forming marine phytoplankton. *Limnology and Oceanography*, 48(1), p. 55-67.

Schefuβ, E., Ratmeyer, V., Stuut, J., Jansen, J. H., Sinninghe Damsté, J. , (2003) Carbon isotope analyses of n-alkanes in dust from the lower atmosphere over the central eastern Atlantic. *Geochemica et Cosmochemica Acta*, 67(10), p. 1757-1767.

Schidlowski, M., (2001) Carbon isotopes as biogeochemical recorders of life over 3.8 Ga of Earth history: evolution of a concept. *Precambrian Research*, 106, p.117-134.

Sinha, A., Stott, L., (1994) New atmospheric pCO_2 estimates from paleosols during the Late Paleocene / Early eocene global warming interval. *Global and planetary change*, 9, p. 297-307.

Stefanova, M., (2004) Molecular indicators for *Taxodium dubium* as coal progenitor of "Chukurovo" lignite, Bulgaria. *Bulletin of the Geological Society of Greece*, 36, p. 342-347.

Stern, L., Johnson, G., Chamberlain, C., (1994) Carbon isotope signature of environmental change found in fossil ratite eggshells from a south Asian Neogene sequence. *Geology*, 22, p. 419-422. .

Strauss, H., peters-Kottig, W., (2003) The Paleozoic to Mesozoic carbon cycle revisited: the carbon isotopic composition of terrestrial organic matter. *Geochemistry, Geophysics, Geosystems*, 4(10), p. 1-15.

Sukh, D., (1989) *Natural Products of Woody Plants,*1. Springer, Berlin. p. 691-807.

Thomas , D., Zachos, J., Bralower, T., Thomas, E., Bohaty, S., (2002) Warming the fuel for the fire: evidence for the thermal dissociation of methane hydrate during the Paleocene-Eocene thermal maximum. *Geology*, 30(12), p.1067-1070.

Tissot, B., Welte., D., (1984) *Petroleum formation and occurrence. Springer-Verlag, New york,* p. 699.

Tuo, J., Philp, R. P., (2005) Saturated and aromatic diterpenoids and triterpenoids in Eocene coals and mudstones from China. *Applied Geochemistry*, 20, p. 367-381.

Utescher, T., Mosbrugger, V., Ashraf, A., (2000) Terrestrial climate evolution in northwest Germany over the last 25 million years. *Palaios*, 15, p. 430-449.

van Breugel, Y., (2006) Causes for negative carbon isotope anomalies in Mesozoic marine sediments: constraints from modern and ancient anoxic settings. *Geologica Ultraiectina*, 258, p. 9-18.

Veizer, J., Ala, D., Azmy, K., Bruckschen, P., Buhl, D., Bruhn, F., Carden, G., Diener, A., Ebneth, S., Godderis, Y., Jasper, T., Korte, C, Pawellek, F., Podlaha, O., Strauss, H., (1999) ^{87}Sr / ^{86}Sr, $\delta^{13}C$ and $\delta^{18}O$ evolution of Phanerozoic seawater. *Chemical Geology*, 161, p. 59-88.

Villamil, T., (1999) Campanian-Miocene tectonostratigraphy, depocenter evolution and basin development of Colombia and western Venezuela. *Palaeogeography, Palaeoclimatology, Palaeoecology*, 153, p. 239-275.

Weissert, H., Lini, A., Föllmi, K., Kuhn, O., (1998) Correlation of Early Cretaceous carbon isotope stratigraphy and platform drowning events; a possible link? *Palaeogeography, Palaeoclimatology, Palaeoecology*, 137, p. 189-203.

Weissert, H., Erba, E., (2004) Volcanism, CO_2 and palaeoclimate: a Late Jurassic-Early Cretaceous carbon and oxygen isotope records. *Journal of the Geological Society, London*, 161, p. 695-702.

Zachos, J., Pagani, M., Sloan, L., Thomas, E., Billups, K., (2001) Trends, rhytms and aberrations in global climate 65 M.a. to present. *Science*, 292, p. 686-693.

APPENDIX 1. RAW DATA FOR $\delta^{13}C_{bulk}$ VALUES AND BIOMARKER RATIOS

DEPTH feet	meters	Age (m.a.)	Formation	Organic carbon (wt.%)	$\delta^{13}C_{bulk}$ (‰ PDB) Gonzalez-1	Asphaltenes (mg/g C_{org})	CPI	Pr/Ph	Paq	ββ/(ββ+αβ) Hopanes
530-540	161.544	50.06542	Mirador	0.2	-26.080					
580-590	164.592	50.39252	Mirador	0.41	-25.961					
590-600	167.64	50.45794	Cuervos	0.62	-25.824					
600-610	170.688	50.52336	Cuervos	0.37	-22.018					
610-620	173.736	50.58879	Cuervos	3.1	-24.853					
620-630	176.784	50.65421	Cuervos	4.2	-25.486	1.06		**3.49**		
650-660	179.832	50.71963	Cuervos	3.44	-23.821					
670-680	182.88	50.85047	Cuervos	0.66	-28.861					
680-690	185.928	50.98131	Cuervos	6.82	-25.450					
690-700	188.976	51.11215	Cuervos	6.25	-25.938					
700-710	192.024	51.17757	Cuervos	4.34	-25.774	26.43		**2.6**		
710-720	195.072	51.24299	Cuervos	3.92	-25.008					
720-730	198.12	51.43925	Cuervos	2.66	-26.003					
740-750	204.216	51.63551	Cuervos	1.42	-26.112					
760-770	210.312	51.83178	Cuervos	0.93	-26.725					
780-790	216.408	52.02804	Cuervos	0.28	-27.125					
790-800	219.456	52.2243	Cuervos	0.31	-26.977	3.21				
800-830	228.6	52.42056	Cuervos	1.92	-26.512					
830-860	237.744	52.61682	Cuervos	0.43	-26.810					
860-890	246.888	52.81308	Cuervos	0.17	-26.870					
890-920	256.032	53.00935	Cuervos	0.19	-26.117					
920-950	265.176	53.20561	Cuervos	0.51	-26.291					
950-980	274.32	53.40187	Cuervos	0.33	-27.091					
980-1010	283.464	53.59813	Cuervos	0.23	-27.997					
1010-1040	292.608	53.79439	Cuervos	0.26	-26.998	30.65		**2.2**		
1040-1070	301.752	53.99065	Cuervos	0.16	-26.849					
1070-1100	310.896	54.18692	Cuervos	0.18	-25.872					
1100-1130	320.04	54.38318	Cuervos	0.0065	-26.356					
1130-1160	329.184	54.57944	Cuervos	0.1	-24.750					
1160-1190	338.328	54.97196	Cuervos	0.14	-26.421					
1190-1220	347.472	55.16822	Cuervos	0.47	-26.622	8.81	**1.27**	**2.6**	**0.67**	0.27
1220-1250	356.616	55.36449	Cuervos	0.12	-26.249					
1280-1310	365.76	55.56075	Cuervos	0.18	-26.045					
1310-1340	374.904	55.75701	Cuervos	0.41	-25.753	26.43	**1.33**		**0.67**	0.5
1370-1400	384.048	55.95327	Cuervos	0.74	-26.067					
1430-1460	393.192	56.14953	Cuervos	3.26	-24.920					
1460-1490	402.336	56.34579	Cuervos	11.24	-21.206	15.28	**1.24**	**1.28**	**0.69**	0.33
1520-1550	411.48	56.54206	Cuervos	10.77	-23.523					
1550-1580	420.624	56.73832	Cuervos	5.57	-23.905	1.34				
1580-1610	429.768	56.93458	Cuervos	0.59	-24.428					
1610-1640	438.912	57.13458	Cuervos	0.77	-26.095					
1640-1670	448.056	57.33458	Barco	0.25	-29.969					

DEPTH feet	meters	Age (m.a.)	Formation	Organic carbon (wt.%)	$\delta^{13}C_{bulk}$ (‰ PDB) Gonzalez-1	Asphaltenes (mg/g C_{org})	CPI	Pr/Ph	Paq	ββ/(ββ+αβ) Hopanes
1670-1700	457.2	57.53458	Barco	1	-26.702	43.57	**1.52**	**1.83**	**0.8**	0.37
1700-1730	466.344	57.73458	Barco	0.67	-24.496					
1730-1760	475.488	57.93458	Barco	1.28	-25.583					
1760-1790	484.632	58.13458	Barco	0.53	-25.762					
1790-1820	493.776	58.33458	Barco	0.34	-26.042					
1820-1850	502.92	58.53458	Barco	4.03	-23.671	14.98	**1.52**	**2.45**	**0.64**	0.3
1850-1880	512.064	58.73458	Barco	0.49	-26.114					
1880-1910	521.208	58.93458	Barco	0.33	-26.179					
1910-1940	530.352	59.16185	Barco	0.54	-26.499					
1940-1970	539.496	59.38912	Catatumbo	0.38	-25.985					
1970-2000	548.64	59.6164	Catatumbo	2.71	-25.908		**1.31**	**1.45**	**0.77**	0.1
2000-2030	557.784	59.84367	Catatumbo	2.38	-25.831	3.21	**1.63**	**4.59**	**0.7**	0.22
2060-2090	566.928	60.07094	Catatumbo	1.42	-24.370					
2120-2150	576.072	60.29822	Catatumbo	0.43	-25.770					
2150-2180	585.216	60.52549	Catatumbo	0.67	-27.154					
2180-2210	594.36	60.75276	Catatumbo	3.1	-26.319	12.83	**1.67**	**4.3**	**0.75**	0.23
2210-2240	603.504	60.98003	Catatumbo	6.77	-24.659					
2240-2270	612.648	61.20731	Catatumbo	1.84	-23.913					
2270-2300	621.792	61.43458	Catatumbo	4.77	-24.778					
2300-2330	630.936	61.66185	Catatumbo	1.21	-25.036	25.93	**1.92**	**1.96**	**0.97**	
2330-2360	640.08	61.88912	Catatumbo	0.77	-26.497					
2360-2390	649.224	62.1164	Catatumbo	0.74	-22.278		**1.65**	**3.33**	**0.8**	
2390-2420	658.368	62.34367	Catatumbo	2.65	-23.846					
2450-2480	667.512	62.57094	Catatumbo	0.45	-23.032					
2480-2510	676.656	62.79822	Catatumbo	0.71	-24.175					
2510-2540	685.8	63.02549	Catatumbo	1.68	-26.403	26.74	**1.54**	**0.94**	**0.8**	0.3
2570-2580	694.944	63.25276	Catatumbo	0.77	-25.975					

Depth		Age (m.a.)	Formation	$\delta^{13}C_{bulk}$ (‰ PDB)	Asphaltenes (mg/g C_{0rg})	CPI	Pr/Ph	Paq	ββ/(ββ+αβ) Hopanes
feet	meters			Diablito-1					
896.0	273.1	57	Cuervos	-26.160					
930.9	283.7	57.12	Barco	-26.469					
949.8	289.5	57.39	Barco	-25.918					
988.8	301.4	57.59	Barco	-25.753					
1018.5	310.4	57.82	Barco	-25.109					
1052.3	320.7	58.01	Barco	-26.407					
1079.4	329.0	58.23	Barco	-26.589					
1112.2	339.0	58.42	Barco	-26.639					
1140.3	347.6	58.69	Barco	-25.554					
1179.6	359.5	58.98	Barco	-25.720	5.12	2.11	2.79	0.68	0.27
1221.0	372.2	59.17	Barco	-25.865					
1249.2	380.8	59.42	Catatumbo	-25.744					
1286.4	392.1	59.57	Catatumbo	-26.081					
1307.9	398.6	59.86	Catatumbo	-25.189					
1349.7	411.4	60.05	Catatumbo	-26.771					
1379.0	420.3	60.29	Catatumbo	-25.904					
1413.3	430.8	60.46	Catatumbo	-27.025					
1438.0	438.3	60.73	Catatumbo	-25.319					
1478.5	450.6	61	Catatumbo	-25.839					
1517.5	462.5	61.22	Catatumbo	-26.202					
1550.3	472.5	61.41	Catatumbo	-25.776	43.83	1.93		0.64	0.22
1574.1	479.8	61.6	Catatumbo	-25.887					
1599.5	487.5	61.65	Catatumbo	-25.156	3.76	1.6	2.02	0.49	0.24
1605.8	489.4	61.68	Catatumbo	-24.858					
1610.5	490.9	61.9	Catatumbo	-25.605					
1638.2	499.3	61.92	Catatumbo	-25.391	5.95	1.67	2.19	0.75	0.33
1641.3	500.3	61.96	Catatumbo	-25.325	27.45	2.47	1.94	0.72	0.26
1646	501.7	62.02	Catatumbo	-25.133					
1654.5	504.3	62.15	Catatumbo	-25.719					
1671.0	509.3	62.16	Catatumbo	-25.922					
1672.8	509.9	62.26	Catatumbo	-25.557	17.56	1.84		0.57	0.14
1685.5	513.7	62.42	Catatumbo	-25.835					
1706.0	520.0	62.43	Catatumbo	-26.730					
1707.7	520.5	62.5	Catatumbo	-25.828					
1716.4	523.2	62.58	Catatumbo	-25.204					
1727.1	526.4	62.62	Catatumbo	-25.866					
1731.8	527.9	62.63	Catatumbo	-25.298					
1732.1	527.9	62.71	Catatumbo	-25.798					
1744	531.6	62.76	Catatumbo	-25.349					
1750.5	533.6	62.77	Catatumbo	-25.781	22.36	1.93		0.55	0.31
1751.7	533.9	62.78	Catatumbo	-25.532					
1752.9	534.3	62.82	Catatumbo	-25.751					

1758.3	535.9	62.84	Catatumbo	-25.613					
1761.4	536.9	62.87	Catatumbo	-26.17					
Depth		**Age (m.a.)**	**Formation**	**$\delta^{13}C_{bulk}$ (‰ PDB)**	**Asphaltenes (mg/g C_{0rg})**	**CPI**	**Pr/Ph**	**Paq**	**ββ/(ββ+αβ) Hopanes**
feet	**meters**			**Diablito-1**					
1765.3	538.1	62.94	Catatumbo	-25.426					
1774.2	540.8	63.04	Catatumbo	-25.047					
1787.2	544.7	63.06	Catatumbo	-25.252					
1789.5	545.4	63.12	Catatumbo	-25.966					
1797.9	548.0	63.13	Catatumbo	-25.34	4.03	1.7	0.81	0.83	0.24
1799.1	548.4	63.3	Catatumbo	-25.774					
1821.5	555.2	63.52	Catatumbo	-26.107					
1849.4	563.7	63.79	Catatumbo	-26.158					
1885.2	574.6	64.22	Catatumbo	-26.099					
1941.4	591.7	64.41	Catatumbo	-25.858					
1965.5	599.1	64.61	Catatumbo	-26.047					
1991.0	606.9	64.81	Catatumbo	-25.824					
2018.0	615.1	65.16	Catatumbo	-25.954					
2062.9	628.8	65.42	Catatumbo	-25.258					
2097.1	639.2	65.54	Catatumbo	-25.379					
2113.0	644.0	65.81	Catatumbo	-25.814					
2147.7	654.6	66.24	Catatumbo	-24.660					
2204.2	671.8	66.55	Catatumbo	-24.532					
2244.4	684.1	66.74	Catatumbo	-25.030					
2269.4	691.7	66.97	Catatumbo	-24.303					
2299.2	700.8	67	Catatumbo	-24.915					

APPENDIX 2. RELATIVE ABUNDANCES FOR THE IDENTIFIED COMPONDS

No.	Name	MW	Composition	Diablito-1				
				R. A.*				
				Geol 1	Geol 2	Geol 3	Geol 5	Geol 6
	n-Alkanes and Isoprenoids			**359.5****	**472.5**	**487.5**	**499.3**	**500.3**
nC_{13}	n-Tridecane	184	$C_{13}H_{28}$	0	7.13	12.55	23.12	29.38
nC_{14}	n-Tetradecane	198	$C_{14}H_{30}$	77.52	42.2	37.65	71.88	82.19
nC_{15}	n-Pentadecane	212	$C_{15}H_{32}$	42.95	27.99	74.08	100	58.12
nC_{16}	n-Hexadecane	226	$C_{16}H_{34}$	100	43.3	100	70.88	100
nC_{17}	n-Heptadecane	240	$C_{17}H_{36}$	80.34	100	78.94	37.87	54.38
nC_{18}	n-Octadecane	254	$C_{18}H_{38}$	58.15	27.16	42.51	21.11	52.26
nC_{19}	n-Nonadecane	268	$C_{19}H_{40}$	26.3	17.9	29.95	10.03	23.9
nC_{20}	n-Eicosane	282	$C_{20}H_{42}$	21.46	16.37	17	8.95	17.87
nC_{21}	n-Heneicosane	296	$C_{21}H_{44}$	20.02	17.87	17.81	5.79	17.32
nC_{22}	n-Docosane	310	$C_{22}H_{46}$	16.01	14.5	19.43	3.93	11.23
nC_{23}	n-Tricosane	324	$C_{23}H_{48}$	18.51	15.65	20.24	4.4	11.57
nC_{24}	n-Tetracosane	338	$C_{24}H_{50}$	13.8	14.55	21.45	3.08	6.5
nC_{25}	n-Pentacosane	352	$C_{25}H_{52}$	15.15	15.2	17	2.25	5.68
nC_{26}	n-Hexacosane	366	$C_{26}H_{54}$	9.75	12.6	18.21	1.96	4.65
nC_{27}	n-Heptacosane	380	$C_{27}H_{56}$	15.31	15.92	21.86	2	4.72
nC_{28}	n-Octacosane	394	$C_{28}H_{58}$	7.62	8.26	18.21	1.05	2.26
nC_{29}	n-Nonacosane	408	$C_{29}H_{60}$	10.52	12.98	25.1	1.17	4.11
nC_{30}	n-Triacontane	422	$C_{30}H_{62}$	4.26	4.6	11.33	0.8	0
nC_{31}	n-Hentriacontane	436	$C_{31}H_{64}$	5.69	5.06	12.55	0.92	2.53
nC_{32}	n-Dotriacontane	450	$C_{32}H_{66}$	0		0	0	0
nC_{33}	n-Tritriacontane	464	$C_{33}H_{68}$	0	0	0	0	0
Pr	Pristane	268	$C_{19}H_{40}$	77.8	0	85.02	30.87	39.72
Ph	Phytane	282	$C_{20}H_{42}$	28.62	14.53	42.1	14.12	20.47
	Sesquiterpenoids							
Tp_1	Bicyclic sesquiterpane	222	$C_{16}H_{30}$	10.81	5.51	18.21	10.88	27.12
Tp_2	Cadalene	198	$C_{15}H_{18}$	27.68	9.1	6.88	62.7	59.72
	Triterpenoids							
L_1	Normoretane	398	$C_{29}H_{50}$	16.17	10.99	10.12	0.97	3.63
L_2	Lupane (Oleanane?)	412	$C_{30}H_{52}$	48.61	17.38	25.1	3.01	3.76
	Hopanoids							
H_1	17α-22,24,30-Trisnorhopane	370	$C_{27}H_{46}$	21.82	19.68	14.57	1.58	5.41
H_2	17α(H),21β(H)-Hopane	398	$C_{29}H_{50}$	38.74	25.12	25.5	3.23	7.74

H_3	17α,21β(H)-Norhopane	398 $C_{29}H_{50}$	5.28	6.82	7.69	0.6	4.18
H_4	17β(H),21β(H)-Hopane	412 $C_{30}H_{52}$	14.25	7.18	8.09	1.12	0
H_5	17α(H),21β(H)-Homohopane	426 $C_{31}H_{54}$				1.5	0
H_6	17β(H),21β(H)-Homohopane	426 $C_{31}H_{54}$					0
H_7	C_{32} Hopanoid	440 $C_{32}H_{56}$				1.17	2.8
H_8	17α(H),21β(H)-Trishomohopane	454 $C_{33}H_{58}$					

* R. A.=Relative Abundance.
**Values under the name of the sample correspond to the depth in meters.

No.	Name	MW	Composition	R. A.*	Diablito-1	
				Geol 7	Geol 8	Geol 9
	n-Alkanes and Isoprenoids			**509.9**	**533.6**	**548**
nC_{13}	n-Tridecane	184	$C_{13}H_{28}$	24.19	0	50.02
nC_{14}	n-Tetradecane	198	$C_{14}H_{30}$	42.67	10.86	81.99
nC_{15}	n-Pentadecane	212	$C_{15}H_{32}$	49.2	12.97	100
nC_{16}	n-Hexadecane	226	$C_{16}H_{34}$	51.96	26.05	89.7
nC_{17}	n-Heptadecane	240	$C_{17}H_{36}$	100	100	79.07
nC_{18}	n-Octadecane	254	$C_{18}H_{38}$	15.88	9.91	63.96
nC_{19}	n-Nonadecane	268	$C_{19}H_{40}$	16	9.7	48.5
nC_{20}	n-Eicosane	282	$C_{20}H_{42}$	10.8	8.07	38.72
nC_{21}	n-Heneicosane	296	$C_{21}H_{44}$	12.46	10.55	31.2
nC_{22}	n-Docosane	310	$C_{22}H_{46}$	11.53	9.6	24.31
nC_{23}	n-Tricosane	324	$C_{23}H_{48}$	9.94	9.4	16.79
nC_{24}	n-Tetracosane	338	$C_{24}H_{50}$	9.9	8.86	11.9
nC_{25}	n-Pentacosane	352	$C_{25}H_{52}$	10.33	9.4	7.37
nC_{26}	n-Hexacosane	366	$C_{26}H_{54}$	8.15	7.23	4.69
nC_{27}	n-Heptacosane	380	$C_{27}H_{56}$	10.21	9.86	3.26
nC_{28}	n-Octacosane	394	$C_{28}H_{58}$	6.48	5.91	2.47
nC_{29}	n-Nonacosane	408	$C_{29}H_{60}$	8.77	10.1	2.9
nC_{30}	n-Triacontane	422	$C_{30}H_{62}$	4.74	4.48	2.01
nC_{31}	n-Hentriacontane	436	$C_{31}H_{64}$	6.29	4.8	2.06
nC_{32}	n-Dotriacontane	450	$C_{32}H_{66}$	0	0	0
nC_{33}	n-Tritriacontane	464	$C_{33}H_{68}$	0	0	0
Pr	Pristane	268	$C_{19}H_{40}$	0	0	17.65
Ph	Phytane	282	$C_{20}H_{42}$	12.9	10.17	21.8
	Sesquiterpenoids					
Tp_1	Bicyclic sesquiterpane	222	$C_{16}H_{30}$	20.58	25	12.6
Tp_2	Cadalene	198	$C_{15}H_{18}$	43.8	35.97	18.86
	Triterpenoids					
L_1	Normoretane	398	$C_{29}H_{50}$	5.51	4.37	0.6
L_2	Lupane (Oleanane?)	412	$C_{30}H_{52}$	9.71	7.4	2.96

	Hopanoids				
H_1	17α-22,24,30-Trisnorhopane	370 $C_{27}H_{46}$	12.04	8.4	1.3
H_2	17α(H),21β(H)-Hopane	398 $C_{29}H_{50}$	15.22	8.38	3.2
H_3	17α,21β(H)-Norhopane	398 $C_{29}H_{50}$	4.7	1.68	0
H_4	17β(H),21β(H)-Hopane	412 $C_{30}H_{52}$	0	3.22	0.44
H_5	17α(H),21β(H)-Homohopane	426 $C_{31}H_{54}$	4.81	3.64	1.06
H_6	17β(H),21β(H)-Homohopane	426 $C_{31}H_{54}$	0		0
H_7	C_{32} Hopanoid	440 $C_{32}H_{56}$	3.34	2.22	0.89
H_8	17α(H),21β(H)-Trishomohopane	454 $C_{33}H_{58}$			

* R. A.=Relative Abundance.
**Values under the name of the sample correspond to the depth in meters.

No.	Name	MW	Composition	Gonzalez-1				
				R. A.*				
				Geol 11	Geol 12	Geol 14	Geol 15	Geol 16
	n-Alkanes and Isoprenoids			**176.78****	**192.02**	**292.6**	**347.47**	**374.9**
nC_{13}	n-Tridecane	184	$C_{13}H_{28}$	0	0	0	0	0
nC_{14}	n-Tetradecane	198	$C_{14}H_{30}$	42.01	40.77	33.54	40.02	100
nC_{15}	n-Pentadecane	212	$C_{15}H_{32}$	94.56	76.61	62.69	63.68	98.07
nC_{16}	n-Hexadecane	226	$C_{16}H_{34}$	100	100	100	100	94.25
nC_{17}	n-Heptadecane	240	$C_{17}H_{36}$	54.97	42.72	53.29	36.72	49.98
nC_{18}	n-Octadecane	254	$C_{18}H_{38}$	51.65	66.61	52.5	33.37	74.98
nC_{19}	n-Nonadecane	268	$C_{19}H_{40}$	0	4.67	10.66	4.14	14.61
nC_{20}	n-Eicosane	282	$C_{20}H_{42}$	13.52	26.38	6.64	4.86	23.21
nC_{21}	n-Heneicosane	296	$C_{21}H_{44}$	0	0	0	1.02	8.6
nC_{22}	n-Docosane	310	$C_{22}H_{46}$	1.98	0	0	1.43	10.29
nC_{23}	n-Tricosane	324	$C_{23}H_{48}$	0	0	0	1.03	7.95
nC_{24}	n-Tetracosane	338	$C_{24}H_{50}$	0	0	0	0.86	5.53
nC_{25}	n-Pentacosane	352	$C_{25}H_{52}$	0	0	0	0.82	4.4
nC_{26}	n-Hexacosane	366	$C_{26}H_{54}$	0	0	0	0.79	4.27
nC_{27}	n-Heptacosane	380	$C_{27}H_{56}$	0	0	0	0.59	4.36
nC_{28}	n-Octacosane	394	$C_{28}H_{58}$	0	0	0	0.63	3.3
nC_{29}	n-Nonacosane	408	$C_{29}H_{60}$	0	0	0	0.45	3.83
nC_{30}	n-Triacontane	422	$C_{30}H_{62}$	0	0	0	0.38	1.95
nC_{31}	n-Hentriacontane	436	$C_{31}H_{64}$	0	0	0	0.44	2.16
nC_{32}	n-Dotriacontane	450	$C_{32}H_{66}$	0	0	0	0	0.76
nC_{33}	n-Tritriacontane	464	$C_{33}H_{68}$	0	0	0	0	0
Pr	Pristane	268	$C_{19}H_{40}$	30.67	23.57	37.95	17.13	0
Ph	Phytane	282	$C_{20}H_{42}$	8.77	9.1	17.28	6.6	9.87
	Sesquiterpenoids							
Tp_1	Bicyclic sesquiterpane	222	$C_{16}H_{30}$	10.11	30.85	10.01	2.68	22.62
Tp_2	Cadalene	198	$C_{15}H_{18}$	9.46	35.87	13.61	8.26	10.97
	Triterpenoids							
L_1	Normoretane	398	$C_{29}H_{50}$	0	0	0.09	0	3.34
L_2	Lupane (Oleanane?)	412	$C_{30}H_{52}$	0	0	0.54	0.48	10.49
					0			

	Hopanoids			0			
H_1	17α-22,24,30-Trisnorhopane	370 $C_{27}H_{46}$	0	0	0.4	0.45	8.71
H_2	17α(H),21β(H)-Hopane	398 $C_{29}H_{50}$	0	0	0.46	0.45	16.23
H_3	17α,21β(H)-Norhopane	398 $C_{29}H_{50}$	0	0	0	0	0
H_4	17β(H),21β(H)-Hopane	412 $C_{30}H_{52}$	0	0	0	0	3.08
H_5	17α(H),21β(H)-Homohopane	426 $C_{31}H_{54}$	0	0	0	0	2.6
H_6	17β(H),21β(H)-Homohopane	426 $C_{31}H_{54}$	0	0	0	0	2.61
H_7	C_{32} Hopanoid	440 $C_{32}H_{56}$	0	0	0	0	1.32
H_8	17α(H),21β(H)-Trishomohopane	454 $C_{33}H_{58}$					

* R. A.=Relative Abundance.
**Values under the name of the sample correspond to the depth in meters.

No.	Name	MW	Composition	Gonzalez-1				
				R. A.*				
				Geol 17	Geol 19	Geol 21	Geol 22	Geol 23
	n-Alkanes and Isoprenoids			**402.33****	**457.2**	**502.92**	**548.64**	**557.78**
nC_{13}	n-Tridecane	184	$C_{13}H_{28}$	0	0	0	90.17	0
nC_{14}	n-Tetradecane	198	$C_{14}H_{30}$	0	45.3	20.93	99.69	80.42
nC_{15}	n-Pentadecane	212	$C_{15}H_{32}$	0	58.11	40.87	94.06	78.43
nC_{16}	n-Hexadecane	226	$C_{16}H_{34}$	93.16	100	97.72	94.04	100
nC_{17}	n-Heptadecane	240	$C_{17}H_{36}$	100	25.97	65.3	95.29	51.24
nC_{18}	n-Octadecane	254	$C_{18}H_{38}$	55.61	65.36	26.93	93.63	62.79
nC_{19}	n-Nonadecane	268	$C_{19}H_{40}$	63.63	12.59	90.15	98.08	21.05
nC_{20}	n-Eicosane	282	$C_{20}H_{42}$	75.31	18.39	56.26	99.02	27.89
nC_{21}	n-Heneicosane	296	$C_{21}H_{44}$	78.19	3.09	50.82	100	18.06
nC_{22}	n-Docosane	310	$C_{22}H_{46}$	65.92	7.16	0	94.59	17.72
nC_{23}	n-Tricosane	324	$C_{23}H_{48}$	63.87	5.89	61.38	97.73	16.92
nC_{24}	n-Tetracosane	338	$C_{24}H_{50}$	38.07	2.27	35.82	93.37	12.4
nC_{25}	n-Pentacosane	352	$C_{25}H_{52}$	46.96	1.96	38.44	94.58	10.73
nC_{26}	n-Hexacosane	366	$C_{26}H_{54}$	54.27	1.55	38.75	92.13	8.29
nC_{27}	n-Heptacosane	380	$C_{27}H_{56}$	45.71	1.52	45.57	87	7.09
nC_{28}	n-Octacosane	394	$C_{28}H_{58}$	38.27	1.25	31.7	75.96	4.95
nC_{29}	n-Nonacosane	408	$C_{29}H_{60}$	32.68	1.19	36.41	53.73	5.21
nC_{30}	n-Triacontane	422	$C_{30}H_{62}$	24.61	0.68	17.31	12.57	2.32
nC_{31}	n-Hentriacontane	436	$C_{31}H_{64}$	17.63	0.62	17.75	1.8	2.41
nC_{32}	n-Dotriacontane	450	$C_{32}H_{66}$	5.14	0	6.51	0	0
nC_{33}	n-Tritriacontane	464	$C_{33}H_{68}$	3.45	0	4.81	0	0
Pr	Pristane	268	$C_{19}H_{40}$	89.4	12.71	51.18	77.53	55.94
Ph	Phytane	282	$C_{20}H_{42}$	47.48	6.95	20.86	53.43	12.18
	Sesquiterpenoids							
Tp_1	Bicyclic sesquiterpane	222	$C_{16}H_{30}$	0	5.27	13.87	22.99	10.76
Tp_2	Cadalene	198	$C_{15}H_{18}$	0	0.87	8.48	39.51	7.04
	Triterpenoids							
L_1	Normoretane	398	$C_{29}H_{50}$	25.02	0.73	12.38	30.01	2.49
L_2	Lupane (Oleanane?)	412	$C_{30}H_{52}$	43.38	5.16	100	98	11.75

	Hopanoids						
H_1	17α-22,24,30-Trisnorhopane	370 $C_{27}H_{46}$	34.23	1.58	31.59	89.23	7.07
H_2	17α(H),21β(H)-Hopane	398 $C_{29}H_{50}$	37.33	4.54	91.51	94.8	17.035
H_3	17α,21β(H)-Norhopane	398 $C_{29}H_{50}$	12.73	0.33	4.66	7.24	2.79
H_4	17β(H),21β(H)-Hopane	412 $C_{30}H_{52}$	39.65	1.45	37.38	30.76	0
H_5	17α(H),21β(H)-Homohopane	426 $C_{31}H_{54}$	44.66	1.46	26.99	44.69	2.96
H_6	17β(H),21β(H)-Homohopane	426 $C_{31}H_{54}$	17.77	0	2.06	8.49	0.7
H_7	C_{32} Hopanoid	440 $C_{32}H_{56}$	36.52	1.52	38.6	24.27	1.5
H_8	17α(H),21β(H)-Trishomohopane	454 $C_{33}H_{58}$	12.01	0	11.44	6.09	0

* R. A.=Relative Abundance.
**Values under the name of the sample correspond to the depth in meters.

No.	Name	MW	Composition	Gonzalez-1			
				R. A.*			
				Geol 24	Geol 25	Geol 26	Geol 27
	n-Alkanes and Isoprenoids			**594.36****	**630.93**	**649.22**	**685.8**
nC_{13}	n-Tridecane	184	$C_{13}H_{28}$	75.76	0	0	0
nC_{14}	n-Tetradecane	198	$C_{14}H_{30}$	100	55.42	49.7	57.22
nC_{15}	n-Pentadecane	212	$C_{15}H_{32}$	90.43	87.7	79.51	72.4
nC_{16}	n-Hexadecane	226	$C_{16}H_{34}$	62.25	100	100	100
nC_{17}	n-Heptadecane	240	$C_{17}H_{36}$	78.79	91.87	53.02	60.31
nC_{18}	n-Octadecane	254	$C_{18}H_{38}$	82.47	93.83	45.42	89.5
nC_{19}	n-Nonadecane	268	$C_{19}H_{40}$	18.81	79.91	13.77	64.49
nC_{20}	n-Eicosane	282	$C_{20}H_{42}$	32.68	90.03	13.57	39.17
nC_{21}	n-Heneicosane	296	$C_{21}H_{44}$	19.66	88.29	7.38	25.35
nC_{22}	n-Docosane	310	$C_{22}H_{46}$	20.33	90.85	7.48	35.88
nC_{23}	n-Tricosane	324	$C_{23}H_{48}$	20.38	94.07	6.75	32.79
nC_{24}	n-Tetracosane	338	$C_{24}H_{50}$	15.61	91.13	5.3	12.31
nC_{25}	n-Pentacosane	352	$C_{25}H_{52}$	13.61	88.01	4.62	8.1
nC_{26}	n-Hexacosane	366	$C_{26}H_{54}$	11.31	55.54	3.47	5.9
nC_{27}	n-Heptacosane	380	$C_{27}H_{56}$	10.79	35.14	3.34	5.39
nC_{28}	n-Octacosane	394	$C_{28}H_{58}$	6.61	10.78	1.83	3.89
nC_{29}	n-Nonacosane	408	$C_{29}H_{60}$	7.81	5.12	1.53	3.23
nC_{30}	n-Triacontane	422	$C_{30}H_{62}$	3.19	0.49	0.97	2.32
nC_{31}	n-Hentriacontane	436	$C_{31}H_{64}$	3.24	0	0.85	1.97
nC_{32}	n-Dotriacontane	450	$C_{32}H_{66}$	0	0	0	0
nC_{33}	n-Tritriacontane	464	$C_{33}H_{68}$	0	0	0	0
Pr	Pristane	268	$C_{19}H_{40}$	77.45	88.4	25.19	40.47
Ph	Phytane	282	$C_{20}H_{42}$	18.03	45.14	7.54	42.96
	Sesquiterpenoids						
Tp_1	Bicyclic sesquiterpane	222	$C_{16}H_{30}$	36.16	28.97	8.83	14.19
Tp_2	Cadalene	198	$C_{15}H_{18}$	15.63	15.76	17.34	26.76
	Triterpenoids						
L_1	Normoretane	398	$C_{29}H_{50}$	6.08	13.84	0.47	5.51
L_2	Lupane (Oleanane?)	412	$C_{30}H_{52}$	23.51	75.58	1.34	46.92

	Hopanoids					
H_1	17α-22,24,30-Trisnorhopane	370 $C_{27}H_{46}$	11.75	35.09	0.89	15.62
H_2	17α(H),21β(H)-Hopane	398 $C_{29}H_{50}$	34.68	89.5	1.97	38.53
H_3	17α,21β(H)-Norhopane	398 $C_{29}H_{50}$	5.33	7.54	0.63	1.91
H_4	17β(H),21β(H)-Hopane	412 $C_{30}H_{52}$	6.48	16.71	0	10.74
H_5	17α(H),21β(H)-Homohopane	426 $C_{31}H_{54}$	7.88	25.22	0.37	7.65
H_6	17β(H),21β(H)-Homohopane	426 $C_{31}H_{54}$	1.73	3.78	0	0
H_7	C_{32} Hopanoid	440 $C_{32}H_{56}$	4.23	14.64	0	9.82
H_8	17α(H),21β(H)-Trishomohopane	454 $C_{33}H_{58}$	0	4.09	0	3.41

* R. A.=Relative Abundance.
**Values under the name of the sample correspond to the depth in meters.

No.	Name	MW	Composition	Identified	Characteristic Fragments
	n-Alkanes and Isoprenoids				
nC_{13}	n-Tridecane	184	$C_{13}H_{28}$	External Standard	85,71
nC_{14}	n-Tetradecane	198	$C_{14}H_{30}$	External Standard	85,71
nC_{15}	n-Pentadecane	212	$C_{15}H_{32}$	External Standard	85,71
nC_{16}	n-Hexadecane	226	$C_{16}H_{34}$	External Standard	85,71
nC_{17}	n-Heptadecane	240	$C_{17}H_{36}$	External Standard	85,71
nC_{18}	n-Octadecane	254	$C_{18}H_{38}$	External Standard	85,71
nC_{19}	n-Nonadecane	268	$C_{19}H_{40}$	External Standard	85,71
nC_{20}	n-Eicosane	282	$C_{20}H_{42}$	External Standard	85,71
nC_{21}	n-Heneicosane	296	$C_{21}H_{44}$	External Standard	85,71
nC_{22}	n-Docosane	310	$C_{22}H_{46}$	External Standard	85,71
nC_{23}	n-Tricosane	324	$C_{23}H_{48}$	External Standard	85,71
nC_{24}	n-Tetracosane	338	$C_{24}H_{50}$	External Standard	85,71
nC_{25}	n-Pentacosane	352	$C_{25}H_{52}$	External Standard	85,71
nC_{26}	n-Hexacosane	366	$C_{26}H_{54}$	External Standard	85,71
nC_{27}	n-Heptacosane	380	$C_{27}H_{56}$	External Standard	85,71
nC_{28}	n-Octacosane	394	$C_{28}H_{58}$	External Standard	85,71
nC_{29}	n-Nonacosane	408	$C_{29}H_{60}$	External Standard	85,71
nC_{30}	n-Triacontane	422	$C_{30}H_{62}$	External Standard	85,71
nC_{31}	n-Hentriacontane	436	$C_{31}H_{64}$	External Standard	85,71
nC_{32}	n-Dotriacontane	450	$C_{32}H_{66}$	External Standard	85,71
nC_{33}	n-Tritriacontane	464	$C_{33}H_{68}$	External Standard	85,71
Pr	Pristane	268	$C_{19}H_{40}$	Philp, 1985	183, 85, 113
Ph	Phytane	282	$C_{20}H_{42}$	Philp, 1985	183, 85, 113
	Sesquiterpenoids				
Tp_1	Bicyclic sesquiterpane	222	$C_{16}H_{30}$	Philp, 1985	123
Tp_2	Cadalene	198	$C_{15}H_{18}$	Philp, 1985	183
	Triterpenoids				
L_1	Normoretane	398	$C_{29}H_{50}$	Philp, 1985	177, 191
L_2	Lupane (Oleanane?)	412	$C_{30}H_{52}$	Philp, 1985	191, 369

	Hopanoids			
H_1	17α-22,24,30-Trisnorhopane	370 $C_{27}H_{46}$	Philp, 1985, Otto et al, 2005	191, 177, 207
H_2	17α(H),21β(H)-Hopane	398 $C_{29}H_{50}$	Philp, 1985, Otto et al, 2005	191, 177, 207
H_3	17α,21β(H)-Norhopane	398 $C_{29}H_{50}$	Philp, 1985, Otto et al, 2005	191, 177, 207
H_4	17β(H),21β(H)-Hopane	412 $C_{30}H_{52}$	Philp, 1985, Otto et al, 2005	191, 177, 207
H_5	17α(H),21β(H)-Homohopane	426 $C_{31}H_{54}$	Philp, 1985, Otto et al, 2005	191, 177, 207
H_6	17β(H),21β(H)-Homohopane	426 $C_{31}H_{54}$	Philp, 1985, Otto et al, 2005	191, 177, 207
H_7	C_{32} Hopanoid	440 $C_{32}H_{56}$	Philp, 1985, Otto et al, 2005	191, 177, 207
H_8	17α(H),21β(H)-Trishomohopane	454 $C_{33}H_{58}$	Philp, 1985, Otto et al, 2005	191, 177, 207